Effects of Soluble Corn Fiber Consumption on Executive Functions and Gut Microbiota in Middle to Older Age Adults: A Randomized Controlled Crossover Trial

David A. Alvarado[1,4*], Tori A. Holthaus[1*], Shelby Martell[2], Nicole L. Southey[1], Marco Atallah[4], Rhea Sarma[3], David Revilla[4], Marina Brown[4], Twinkle Mehta[3], Naiman A. Khan[1,2,3,5], Hannah D. Holscher[1,4**]

[1]Division of Nutritional Sciences, University of Illinois, Urbana-Champaign, Urbana, IL 61801, USA

[2]Neuroscience Program, University of Illinois, Urbana-Champaign, Urbana, IL 61801, USA

[3]Health and Kinesiology, University of Illinois, Urbana-Champaign, Urbana, IL 61801, USA

[4]Department of Food Science and Human Nutrition, University of Illinois, Urbana-Champaign, Urbana, IL 61801, USA

[5]Beckman Institute of Advanced Science and Technology, Urbana-Champaign, Urbana, IL 61801, USA

[*]Shared first-authorship

[**]**Corresponding Author:** Hannah D. Holscher, 1201 West Gregory Drive, Urbana, IL 6180 (217) 300-2512, hholsche@illinois.edu

Clinical Trial Registry: NCT05066425 (https://clinicaltrials.gov/study/NCT05066425)

Abbreviations:

Parabacteroides distasonis (*P. distasonis*), Cambridge Neuropsychological Test Automated Battery (CANTAB), carbohydrate-active enzymes (CAZyme), Event-related potential (ERP), FDR (False Discovery Rate Adjustment, Maltodextrin (CON, control), Perceived Stress Score (PSS), Positive and Negative Affect Schedule (PANAS), Profile of Moods Survey (POMS), Reaction Time (RT), SE (Standard Error), SEM (Standard Error of the Mean), Short-chain fatty acids (SCFA), Branched-chain fatty acids (BCFA), Soluble corn fiber/ PROMITOR® Soluble Fibre™ (SCF)

Abstract

Background: Adequate dietary fiber may support cognitive function through gastrointestinal-microbiota-dependent mechanisms, but evidence from human trials is limited.

Objectives: To determine whether soluble corn fiber (SCF) improves cognition, alters fecal microbiota, and improves fermentation end-product profiles in middle- to older-aged adults with *a priori* aims.

Methods: In this randomized, double-blind, crossover trial, 42 healthy adults (45-75y) consumed SCF (18g/d fiber) or maltodextrin (CON, 22g/d) for 4 weeks, separated by a 4-week washout. Outcomes included executive function (flanker task with event-related potentials), relational memory, neuropsychological testing, mood, fecal microbiota (16S and shotgun sequencing), targeted fecal metabolomics, and gastrointestinal tolerance symptoms. Exploratory analyses tested associations between candidate microbes and metabolites with cognition using correlation, mediation, and moderation models, while microbial species and gene families facilitating SCF fermentation were characterized using predictive metagenomes, *in vitro* culturing, and shotgun metagenomics for a subsample for microbial responder profiling.

Results: *Post-hoc* comparisons indicated that SCF improved reaction times (RT) during congruent (β = -9.65, 95% CI: [-17.4, -1.88], FDR p = 0.01) and incongruent (β = -14.2, 95% CI: [-23.5, -4.95], FDR p = 0.003) flanker trials. SCF also enriched *Parabacteroides* by ~4.1-fold (β = -1.42, 95% CI [-1.74, -1.11], FDR $p < 0.001$). Correlations suggested inverse associations between congruent RT and acetate (ρ = -0.33) and propionate (ρ = -0.36) concentrations, and a positive association between *Parabacteroides* and acetate (ρ = 0.34) (all FDR $p < 0.09$). Moderation analyses suggested exploratory threshold effects of *Parabacteroides* on the SCF-RT response. Predicted metagenome functions were enriched for carbohydrate metabolism pathways and

carbohydrate-active KOs (FDR $p < 0.05$). *In vitro* culturing confirmed *Parabacteroides* fermentation of SCF independent of cross-feeding. Microbial responders exhibited faster RT at baseline and endpoint, alongside greater enrichment of *Parabacteroides* and CAZymes.

Conclusion: SCF consumption improved attentional inhibition, altered fecal microbiota, and primarily enriched *Parabacteroides*. While mediation analyses did not indicate direct microbiota-to-cognition pathways, exploratory findings suggest baseline microbial profiles may shape responsiveness. Collectively, these results highlight SCF as a relevant dietary fiber with potential cognitive benefits in healthy adults.

Keywords: Reaction time; Attentional inhibition; *Parabacteroides*; gut-brain; cognition; fiber; mediation; moderation

Introduction

A healthy diet is a key determinant of metabolic health, and emerging evidence extends these benefits to brain function and cognition [1–3]. Dietary fiber is associated with reduced risk of obesity, cardiovascular disease, type 2 diabetes, and colon cancer [4,5], yet nearly 95% of Americans fail to meet recommended intake levels [6]. Further, dietary fiber provides a primary substrate for microbes residing in the gastrointestinal (GI) tract, shaping ecological community diversity and metabolic capacity [7.] Preclinical studies show that dietary fibers improve cognition [8,9], but human trials remain limited [10–12], particularly those linking the microbiota, GI-derived metabolite,s and cognitive outcomes [13]. Therefore, further evidence is necessary to comprehensively characterize the effect of dietary fiber on general and specific domains of cognitive function.

Soluble corn fiber (SCF) is a resistant maltodextrin with an average degree of polymerization (DP) between 10-12 units [14], that supports glycemic control, calcium retention, and gastrointestinal health [15–17]. Its non-viscous, water-soluble structure lacks β-linkages, yet branching of the α-linkages confers resistance to complete digestion in the small intestine (<30%) [18,19]. The undigested fraction undergoes colonic fermentation, promoting saccharolytic taxa such as *Bifidobacterium*, *Lactobacillus*, and *Parabacteroides* [20,21], increasing production of short-chain fatty acids (SCFA) across age groups [22], while reducing deleterious fermentation-end products (phenols, indoles, ammonia) [19,23]. SCFAs are increasingly recognized as key mediators of GI-brain communications through binding of free fatty acid receptors (FFAR/FFAR3) to regulate immune [24] and enteroendocrine signaling [25], modulating microglial activity and systemic inflammation[26], and stimulating vagal and serotonergic pathways [27–30].

Executive functions, including inhibitory control, are central to attention, working memory, and flexible behavior [31]. These top-down processes can be assessed through computer-

97 based tasks that measure a subject's ability to maintain attention while faced with distracting
98 stimuli, hold and manipulate information in mind, and require multi-tasking and set-shifting, while
99 electrophysiological markers can provide complementary insight into neural activity during such
100 tasks [32,33]. Given the growing evidence that microbially derived metabolites influence brain
101 activity [27,34–39], assessing both behavioral and neural indices provides a comprehensive overview
102 to evaluate dietary fiber's cognitive impact.

103 To address these gaps, we conducted a randomized, double-blind, placebo-controlled,
104 crossover trial to test the impact of daily SCF consumption in middle- to older-aged adults. The
105 primary aim was to determine whether four weeks of SCF consumption improved executive
106 function, changes in the amplitude (size) and latency (timing) of the P3 event-related potential
107 (ERP), as well as additional behavioral tasks assessing relational memory and neuropsychological
108 function. We hypothesized that SCF would enhance cognitive control and reduce the number of
109 neural resources required to accomplish these cognitive processes. The secondary aim examined
110 the effects of SCF on GI microbiota composition and fermentation metabolites, hypothesizing that
111 SCF would enrich health-associated taxa and metabolite profiles. Finally, the tertiary aim tested
112 whether the SCF-induced changes in microbial or metabolite profiles explained changes in
113 cognitive outcomes, hypothesizing that these changes would contribute to the cognitive benefits
114 induced by SCF.

115

116 **Methods**

117 *Study design and intervention*

118 This trial included two 4-week intervention periods separated by a ~4-week washout.
119 Participants consumed either soluble corn fiber (SCF; PROMITOR® Soluble Fibre™, 22g/d

120 containing 18g fiber) or a maltodextrin placebo (CON; 22g/d). The two interventions were
121 provided by Tate & Lyle in identical, pre-measured sachets that were indistinguishable in taste and
122 appearance. Participants and research staff were kept blinded until data analyses were complete.
123 Participants were given 35 sachets per condition and were instructed to consume it daily dissolved
124 in a fluid of choice. Participants recorded intake of the sachet on daily compliance logs. Unused
125 sachets and logs were collected at the end of each period to assess adherence. To minimize learning
126 effects, participants completed practice sessions at the start of each visit until at least 70% accuracy
127 was meet before experimental cognitive sessions were administered. Anthropometric measures,
128 physical activity level, demographic information, and medical history were collected at baseline
129 and visits 4, 5, and 6 as potential covariates. The order of cognitive task administration at each
130 testing visit (visits 3-6) was counterbalanced using a 2x2 Latin square design for each participant,
131 and all study visits and testing sessions were conducted at the University of Illinois at Urbana-
132 Champaign (**Figure 1**).
133
134 *Participants criteria*
135 Adults aged 45-75 years were recruited from the East Central Illinois area using email
136 newsletters, social media, community postings using the postal service, and flyers posted on public
137 transport. All participants were informed of all procedures and provided their written informed
138 consent before any data was collected. The study was approved by the University of Illinois
139 Institutional Review Board (May 2021), registered on ClinicalTrials.gov (NCT05066425), and
140 conducted following the principles of the Declaration of Helsinki.
141 Exclusion criteria included physician-diagnosed gastrointestinal or metabolic disease
142 (inflammatory bowel disease and diabetes), neurological disorder (dementia, Parkinson's disease,

143 multiple sclerosis, brain tumors, autism), colorblindness or vision not corrected to 20/20, antibiotic
144 use within the past month, tobacco use, food allergies, pregnancy, or lactating, BMI <18.5 or >34.9
145 kg/m^2, Mini-Mental State Examination <24, or if habitual dietary fiber intake was >70% of the
146 daily recommended intake (≥18 g/d for women, ≥27 g/d for men) using the Dietary History
147 Questionnaire (*DHQ3*) food frequency questionnaire.

148 Eligible participants agreed to maintain habitual dietary patterns and physical activity, to
149 avoid pro- or prebiotics supplements, and to report any changes in medications during the study.
150 Enrolled participants were randomized via coin toss to start each intervention (i.e., SCF or CON)
151 in a counterbalanced order (**Table 1**) and assigned a study ID by a trained member of the research
152 staff. Sachets were labeled with numeric identifiers to preserve blinding of interventions. Height
153 and weight were measured in triplicate without shoes and in light clothing to determine BMI using
154 a *SECA* stadiometer (model 240; *SECA*, Hamburg, Germany) and Tanita WB-300 Plus digital
155 scale (Tanita, Tokyo, Japan). Physical activity was assessed using the Godin-Shephard Leisure-
156 Time Exercise Questionnaire (*Godin*), which records the frequency of strenuous, moderate, and
157 light physical activities performed during a typical week, which are totaled into a final score using
158 a weighted formula [40].

159

160 **Aim 1: Cognitive Outcomes**

161 *Executive function*

162 Attentional inhibition was assessed using a modified Eriksen flanker task as previously
163 described [41]. Participants were asked to respond (*Current Designs*, Philadelphia, PA, USA) quickly
164 and accurately to the directionality of a central stimulus (3-cm tall white arrow) presented with
165 two flanking stimuli (arrows) on each side (83s stimulus presentation; 100ms response window;

166 jittered intertrial intervals of 1100, 1200, 1500ms). In congruent trial types, the flanking stimuli
167 matched the direction of the central arrow (<<<<<, >>>>>); during incongruent trials, flanking
168 stimuli opposed the central arrow (>><>>, <<><<), requiring greater inhibitory control. The task
169 began with 40 practice trials followed by two blocks of 200 randomized experimental trials.
170 Behavioral measures were accuracy (ACC) and reaction time (RT) for correct responses.
171 Interference effects (flanker effect) for ACC and RT were calculated, respectively, by subtracting
172 incongruent from congruent measures (ACC) and congruent from incongruent measures (RT).
173 These measures index the ability to maintain task performance when resolving conflicting
174 information.
175
176 *Neuroelectric indices*
177 EEG activity was recorded simultaneously during the flanker task via a Neuro-scan Quik-
178 cap with 64 passive, wet, sintered Ag/AgCl scalp electrodes arranged in the international 10–10
179 system, with electrodes placed near the outside of each eye and above and below the left eye [42]. A
180 midline sensor placed between CZ and CPZ served as a reference, and AFZ served as the ground.
181 Continuous EEG data were digitized using a Neuroscan SynampsRT amplifier at a sampling rate
182 of 500 Hz, amplified 500 times to an online low-pass 70-Hz filter with a direct current and a 60-
183 Hz notch filter. Electrode impedance values were maintained at ≤20 kohms.
184 Signal processing was performed in MATLAB (MathWorks, Natick, MA, version 2021b)
185 using EEGLab and ERPlab [43,44]. Continuous data were re-referenced to the average of two mastoid
186 electrodes. A trained research team member visually inspected all channels for excessive noise
187 during pre-processing. Channels with excessive noise were interpolated with an average of the
188 adjacent electrodes. Data were submitted to a 0.1 Hz high-pass Butterworth filter before eye-blink

189 artifacts were rejected using independent component analysis (ICA). ICA and vertical eye sensor
190 channel correlations greater than 0.35 were considered eye-blinks. A time window of -200 to
191 1200 ms around stimulus presentation was used for creating stimulus-locked epochs with a
192 baseline correction of -200 ms to stimulus onset. A 30-Hz low-pass filter was used. Artifacts were
193 detected and rejected if a moving window peak-to-peak amplitude exceeded 100 μV, using a 100-
194 ms window width and step. Only correct trials with >80% of artifact-free trials in all flanker task
195 trials were retained, and participants with excessive artifacts (>20%) were excluded (n = 3 CON,
196 n = 4 SCF), consistent with previous literature [45,46].

197 Electrodes of interest were chosen based on a collapsed localizer technique [47]. Evidence
198 for selection was observed from maximal voltage localization of combined baseline and post-
199 testing trials collapsed across condition and trial type. *Post-hoc* topographic average plots were
200 constructed using a stylized topographic map plugin for EEGLAB/ERPLAB [48]. The P3 component
201 was defined as the region of interest comprised of C1, CZ, C2, CPZ, CP1, and CP2 with a localized
202 peak and corresponding latency between 300 and 600ms post-stimulus onset. Amplitude and
203 latency were extracted to complement the analysis of the behavioral Flanker task.

204

205 *Relational memory*

206 Hippocampal-dependent relational memory was assessed using the computerized spatial
207 reconstruction task presentation software (*iPosition*; Neurobehavioral Systems, Berkeley, CA) [49].
208 Participants studied arrays of six abstract shapes on the computer screen in a randomized array for
209 6 seconds. The shapes were then masked by black squares for 18 seconds and could be revealed
210 individually by clicking on them. After a 2-second delay, the stimuli reappeared at the top of the
211 screen, and participants were asked to reconstruct the original array. Each participant completed

212 20 trials with randomized arrays. Two error metrics were used to assess performance:
213 misplacement error (original misplacement), calculated as the average measure of distance
214 between the actual and reconstructed stimuli locations, and object-location binding (accurate
215 single item placement), the number of times the participant correctly placed a stimulus within a
216 pre-defined radius.
217
218 *Neuropsychological battery*
219 Additional cognitive performance across multiple domains was assessed using the
220 Cambridge Neuropsychological Test Automated Battery (*CANTAB*, Cambridge Cognition Ltd)
221 [50,51], administered on a touchscreen tablet. The battery included the Intra-Extra Dimensional Set
222 Shift (IED), Stop Signal Task (SST), Rapid Visual Information Processing (RVP), and Spatial
223 Working Memory (SWM). The IED is a test which assesses rule acquisition and reversal,
224 attentional set formation, maintenance, and shifting. The RVP task assesses sustained attention,
225 and the SST measures response inhibition. The SWM task assesses spatial working memory.
226
227 *Mood and Stress*
228 Mood and stress were assessed using validated self-report instruments, including the
229 Profile of Mood States (*POMS*), the Positive and Negative Affect Schedule (*PANAS*), and the
230 Perceived Stress Scale (*PSS*). The *POMS* questionnaire includes 65-items that evaluates transient
231 mood states across six subscales (tension/anxiety, depression, anger, vigor, fatigue, and
232 confusion), with ratings from 0 ("not at all") to 5 ("extremely") [52,53]. *PANAS* includes 20 items
233 divided evenly into positive and negative affect subscales, scored from 1 ("very slightly or not at

234 all") to 5 ("extremely likely") [53,54]. *PSS-10* is a 10-item measure of stress over the past month,
235 scored from 0 ("never") to 4 ("very often") [55].
236
237 **Aim 2: Gut Microbiota and Metabolite Outcomes**
238 *Fecal collection and processing*
239 Participants provided two fecal samples at each timepoint, collected during the five days
240 preceding the first intervention and the final five days of each treatment and washout period.
241 Samples were delivered within 15 minutes of defecation using provided kits (Commode Specimen
242 Collection Systems, *Sage Products*) with ice packs, and coolers. Upon arrival at the laboratory,
243 samples were homogenized, aliquoted into cryovials for sequencing, flash-frozen in liquid
244 nitrogen, and stored at -80°C. Additional aliquots were prepared for metabolite analysis: SCFAs,
245 BCFAs, ammonia, and dry matter basis (DMB; pre-weighed aluminum tins). These aliquots were
246 stored at -20°C until analysis. Fecal pH was measured (*Denver Instrument*) after samples have
247 been aliquoted.
248
249 *Fecal DNA isolation and 16S amplicon analyses*
250 Fecal microbial DNA was extracted using the Power-Lyzer PowerSoil DNA Isolation Kit
251 (*QIAGEN*). DNA was verified using 1% agarose gel electrophoresis, concentrations measured
252 using a Qbit 3.0 Fluorometer (*ThermoFisher Scientific*), quantified from two samples collected
253 per timepoint per participant, and pooled in equimolar amounts before sequencing at the University
254 of Illinois W.M Keck Center for Biotechnology. 16S Amplicons were generated with V4 primers
255 (*F*: 5'-GTGYCAGMGCCGCGGTAA, *R*: 5'-GGACTACNVGGGTWTCTAAT) and sequenced
256 on an Illumina NovaSeq 6000 SP (2x250 nt), producing ~1 billion reads. Sequences with quality

257 scores >25 were processed with *DADA2* [56] integrated in *QIIME2* (v2023.7) [57]. Sequences were
258 denoised and resolved into amplicon sequence variants (ASVs) using the *SILVA* 138-99
259 (515F/806R) naïve Bayes reference classifier [56,58]. Samples were normalized to 350,000 reads;
260 curves plateaued at this depth indicating adequate coverage (**Supplemental Figure 1**). Rarefaction
261 was performed with the *vegan* v2.6.8 [59], filtering 1,521 ASVs (13%, primarily singletons or zero-
262 count features) and retaining 10,373 ASVs. Alpha diversity and beta diversity were calculated with
263 *phyloseq* (v1.48.0) [60], and Faiths phylogenetic diversity (PD) with *picante* (v1.8.2). Taxonomic
264 summaries were created at the genus and phylum levels for downstream analyses.
265
266 *Microbial Metabolites*
267 Fecal dry matter was measured according to the Association of Official Analytical
268 Chemists, 1984, methods [61]. Ammonia concentrations were measured following the procedure of
269 Chaney and Marbach [62]. Aliquots for SCFA and BCFA were weighed, acidified with 2N
270 hydrochloric acid, and stored at -20°C until analysis. Before quantification, samples were thawed
271 at room temperature for 15 minutes and centrifuged at 13,000rcf for 10 min, then quantified using
272 gas chromatography mass spectroscopy (GC-MS), normalized by DMB weight [63]. Phenol and
273 indole were quantified, according to Flickinger et al.[64] Fecal metabolites are reported on a DMB
274 scale.
275
276 *Digestive health*
277 GI symptoms, bowel function, and stool characteristics were assessed using 7-day self-
278 reported records, questionnaires, and laboratory measures for each timepoint [65]. Participants rated
279 GI symptom severity (burping, cramping, bloating, gas, nausea, reflux, rumbling) on a 4-point

280 scale from 1 ("absent") to 4 ("severe") [66]. Bowel movements and consistency were scored using a
281 7-point Bristol stool scale (1- "separate hard lumps"; 2- "sausage-shaped but lumpy"; 3- "sausage-
282 like but with cracks on the surface"; 4- "sausage-like, smooth, and soft"; 5- "soft blobs with clear
283 cut edges"; 6- "fluffy pieces, mushy"; 7- "entirely liquid"). And ease of passage rated on a 5-point
284 scale from 1 ("very easy") to 5 ("very difficult"). In the laboratory, fresh fecal samples were
285 measured with a pH meter (Denver Instrument) [65], and a trained research team member recorded
286 stool consistency using the Bristol scale.
287
288 **Aim 3: Integrative and Functional Analyses**
289 Candidate 16S microbial genera and metabolites for integrative analyses were selected
290 based on statistical significance or consistent trends observed in the primary outcomes (Aim 1 and
291 2), with additional consideration informed by prior literature [27,34–39]. Associations between these
292 candidates and cognitive outcomes were examined using Spearman correlations. To assess
293 potential mechanistic pathways, nonparametric bootstrapped causal mediation models estimated
294 indirect and direct effects within a causal inference framework [67–69]. Moderation analyses were
295 conducted using the Johson-Neyman framework with Aiken & West's simple-slopes procedures
296 [70,71]. Together, these complementary approaches helped clarify whether microbial or metabolites
297 acted as intermediaries transmitting the treatment (mediation) or as variables altering the strength
298 or direction of the treatment's effect (moderation).
299
300 *In vitro isolated culturing*
301 *Parabacteroides distasonis* (*P. distasonis*; strain 31_2, deposited as *Porphyromonas* sp.
302 HM-169) was provided from the Biodefense and Emerging Infections Research Resources

303 Repository (BEI Resources, NIAID, NIH) and maintained anaerobically in brain heart infusion
304 (BHI) and chopped-meat broth. Growth assays followed an adaptation of Garcia-Bayona et al. [72]
305 using M9 supplemented with 50 mg/L L-cysteine, 5 mg/L hemin, 2.5 µg/L vitamin K1, 2 mg/L
306 FeSO4·7H2O, 5 µg/L vitamin B12. Treatments included glucose (0.25% wt/vol), CON (0.25%
307 wt/vol), or SCF (0.4% wt/vol). BHI served as a positive control; for negative controls, M9 with no
308 carbon (no growth control), and blanks (no inoculum) for each treatment (media contamination
309 control). Stock solutions were sterile-prepared, filter-sterilized (0.22 µm), and stored at 4 °C.
310 Three separate *P. distasonis* overnight cultures were inoculated into M9 solutions prepared
311 in a 10 x 10 honeycomb plate (1:10 dilution; starting OD_{600} = 0.1). For each treatment there were
312 technical triplicates for each (3) biological replicates. Growth was monitored with the Bioscreen-
313 C system (600nm, every 30 min, for 25.5h, 37 °C, shaking before/after each read) (**Supplemental**
314 **Figure 2**). All samples reached the stationary phase by 14h; therefore, analyses were restricted to
315 the first 14h. OD values were blank-corrected and growth rates (µ) calculated at 2 h intervals.
316
317 *Exploratory metagenomics*
318 Predictive metagenomics for the full cohort were inferred from 16S data using *PICRUSt2*
319 (v2.5.3) [73] with default parameters (*picrust2_pipeline.py*) [73,74]. *KEGGREST* (v112.1) was used to
320 extract carbohydrate metabolism pathways (map00010, 00030, 00500, 00620, 00650) and
321 carbohydrate-active KOs (KO01176, 01223, 01210, 01190, 01187, 012348). Stratified KO files
322 were used to assess genus-level contributions to functional shifts across conditions.
323 Six participants' fecal samples were selected for responder metagenomic analyses from the
324 SCF intervention. Microbial responder status was determined based on changes in
325 *Parabacteroides* abundance following SCF (**Supplemental Figure 3**). Shotgun metagenomic

326 sequencing was performed at the W. M. Keck Center for Biotechnology (University of Illinois
327 Urbana-Champaign). Libraries were pooled, quantified by qPCR, and sequenced on half of a 10B
328 lane for 151 cycles from both ends of the fragments using a NovaSeq X Plus with V1.0 sequencing
329 kits. FastQ files were demultiplexed (*bcl2fastq* v2.20), adapters (CTGTCTCTTATACACATCT)
330 were trimmed from the 3'-end of the reads, and base quality scores were scored using Sanger
331 encoding (*ASCII offset* of 33). Data pre-processing was performed on the University cluster (Carl
332 R. Woese Institute for Genomic Biology, University of Illinois at Urbana-Champaign) using
333 *KneadData* (v0.12.0) for quality control and host DNA removal (*KneadData* 20230405 release).
334 *Trimmomatic* (v0.39) removed low-quality bases, *Tandem Repeat Finder* (TRF) removed noise
335 from repetitive sequences, and *FastQC* (v0.11.9) generated quality reports.

336 Following Huttenhower BioBakery pipelines [75–77], taxonomic profiling was performed
337 using *MetaPhlAn* (v4.0.6) [76], with *Bowtie2* (v2.5.0) aligning reads against the
338 *ChocoPhlAnSGB*_202212 reference. Functional profiles were generated using *HUMAnN* (v3.7) [75]
339 with the *ChocoPhlAn* nucleotide database (v201901b) and *UniRef90* protein database (Nov 2024).
340 Profiles were merged (*merge_metaphlan_tables.py*) to produce relative abundance and read counts
341 [76]. Descriptive analyses compared the log fold change between responders and non-responder's
342 delta values, retaining gene families with >2-fold change targeted filtering for carbohydrate
343 metabolism-related terms yielded 217 candidate families.

344 Carbohydrate-active enzymes (CAZymes) were annotated using the CAZy database [78,79]
345 and *run_dbcan* (v4.0.0)[80], incorporating *HMMER* (*dbCAN_HMMdb)*, *DIAMOND* (CAZy protein
346 sequences), and *dbCAN-sub* for substrate prediction validated against PUL (Polysaccharide
347 Utilization Loci) datasets. Reads were pre-processed (*Trim Galore* v0.6.0, *Kraken2* v2.1.1),
348 assembled into contigs ≥1000 bp (*MEGAHIT* v1.2.9), and annotated with *Prokka* (v1.4) before

349 CAZyme assignment. Clean reads were mapped back to coding sequences (*BWA* v0.7.17-r1188,
350 *Samtools* v1.7, *Bedtools* v2.27.1), and abundances normalized to transcripts per million (TPM)
351 using *dbcan_utils* scripts [80]. Workflow was conducted on a Linux computer (128 GB RAM)
352 utilizing *Anaconda* (v23.7.3) environment.
353

354 **Statistical analyses**

355 *General approach.* Target enrollment was determined using *a priori* power calculations
356 (*G-Power* v3.1.9.2) [81] , estimating that 36 participants would provide 80% power (β =0.80) to
357 detect a small effect size (r = 0.20) at α = 0.05 for Aims 1 and 2. Due to the exploratory nature of
358 Aim 3, results should be interpreted as hypothesis-generating and to inform effect size estimates
359 for future studies. To allow for attrition, 42 participants were recruited. Analyses were conducted
360 in *RStudio* (v2025.05.0+496; *R* v4.4.3) [82]. Significance threshold was set at $\alpha \leq 0.05$ with false
361 discovery rate (FDR) adjustments applied where relevant.

362 *Data preprocessing and assumptions.* Data distributions were checked using Shapiro-
363 Wilk's test (*stats* v4.4.3; $W > 0.9$), Q-Q plots (*ggplot2* v3.5.2) [83], skewness/kurtosis metrics
364 (*DescTools* v0.99.6*, e1071* v2.6*)*, and residuals inspected visually (*performance* v0.13.0). Extreme
365 outliers (>3 SD; *rstatix* v0.7.20) were confirmed using a Bonferroni *outlierTest* (*car* v3.1-3) then
366 winsorized [84,85]. To meet model assumptions, BCFAs POMS, PANAS, and Godin were square
367 root transformed; SCFAs were log-transformed. Data are reported as mean ± SEM unless
368 otherwise noted.

369 *Modeling strategy.* Outcomes were analyzed using linear (*lme4* v1.1.37) or generalized
370 (*glmmTMB* v1.1.11) mixed-effect models with treatment, time, and their interaction as fixed
371 effects with participant ID serving as a random intercept [*Outcome ~ Treatment * Time + (1|ID)*].

372 Order effects were tested and did not improve model fit; demonstrating adequate washout time,
373 therefore excluded. Missing data were not imputed; the mixed-effect model provides valid
374 estimates under the missing-at-random assumption [60]. *Post hoc* pairwise contrasts were estimated
375 with least-square means (*emmeans* v1.11.0) and adjusted with Benjamini-Hochberg corrections.
376 We reported *p*-values, estimates (β), standard error (SE), and 95% confidence intervals (CI; *stats*)
377 for the interaction effect in corresponding **Tables**. Analysis of variance (ANOVA; *lmerTest* v3.1.3,
378 *car* v3.1-3) and *post hoc* summaries were described when interaction effects reached statistical
379 significance. For non-parametric data, paired Wilcoxon Signed-Rank tests were used.

380 *Aim 1*. All measures were analyzed with mixed-effects models (*lme4* v1.1.37). Flanker task
381 measures (ACC, RT, and interference scores) were tested using treatment-by-time models with
382 congruent and incongruent trial types evaluated separately. Two flanker ACC and two P3
383 amplitude outcomes were winsorized; *CANTAB* delta values were compared using paired
384 Wilcoxon Signed-rank tests.

385 *Aim 2*. 16S analyses utilized rarefied counts for normalization. Beta diversity was assessed
386 by PERMANOVA (*vegan* v2.6.10; 5,000 permutations) using participant ID as the permutation
387 stratum, with homogeneity of dispersion (*vegan*, 5,000 permutations) tested in parallel.
388 Differential abundance was assessed with negative binomial mixed-effect models (*glmmTMB*
389 v1.1.11) comparing a null [*Taxa ~ (1|ID)*] and full [*Taxa ~ Treatment * Time + (1|ID)*] model by
390 a likelihood ratio test across all included taxa [86–88]. Alpha diversity and fecal metabolites were
391 analyzed with mixed-effects models (*lme4* v1.1.37). Gastrointestinal symptoms were compared
392 with a paired Wilcoxon Signed-rank test.

393 *Aim 3*. *In vitro* growth rates across treatments were modeled using a linear model (*lm*) with
394 treatment, timepoint (every 2h), and the interaction as fixed effects, followed by *post hoc* pairwise

395 contrasts [89]. Predicted KO and pathway differences were compared with *MaAsLin2* (v1.18.0) [90]
396 and *ggpicrust2* (v2.0.0) [91]. Correlations between cognitive and microbial outcomes were assessed
397 by Spearman rank tests (*stats* v4.4.3). Mediation analysis used baseline-adjusted models to (1)
398 predict the mediator from the Treatment [$\Delta Mediator \sim Treatment + Mediator_{Baseline}$] and (2)
399 predict the outcome from both the Treatment and the Mediator [$\Delta RT \sim Treatment * \Delta Mediator +$
400 $RT_{Baseline}$]. Causal inference was estimated using nonparametric bootstrapping (*mediation* v4.5.0;
401 8,000 simulations) with sensitivity analyses. Reported are the average causal mediation effect
402 (ACME), average direct effect (ADE), total effect, and proportion mediated. Moderation models
403 included treatment, centered-scaled moderator, and its interaction [$\Delta RT \sim Treatment *$
404 $\Delta Moderator_{z\text{-}scaled}$]; participant ID as a random intercept caused model singularity therefore
405 excluded. *Post-hoc* comparisons were probed using simple-slopes (*interactions* v1.2.0) with
406 confidence intervals (*emmeans* v1.11.0) at low (-1 SD), mean, and high (+1 SD) changes of the
407 moderator.
408

409 **Results**

410 *Participant characteristics*

411 The CONSORT diagram (**Figure 2**) summarizes recruitment, enrollment, and retention.
412 Forty-two participants were randomized, of whom 41 completed the trial (**Table 1**). All
413 participants completed at least one cognitive testing visit, including one who withdrew after the
414 first intervention period (n = 1 CON). Per-protocol analyses included compliant participants who
415 consumed >80% of intervention sachets during at least one intervention period (Aim 1; n = 38
416 CON, 39 SCF). Ten participants had unusable P3 amplitude data (n=3 CON; 1 at pre, 2 at post

417 testing) and seven for the SCF (n = 2 pre, 5 post testing). Two participants could not provide fecal
418 samples but completed the primary cognitive aims (Aim 2; n = 38 CON, 37 SCF).
419
420 **Aim 1: Cognitive outcomes**
421 *Executive function*
422 Flanker task ACC was high across all conditions (≥ 92%), with ANOVA showing no
423 treatment by time interactions for congruent (F[1, 112.25] = 0.64, p = 0.42) or incongruent (F[1,
424 110.83] = 0.39, p = 0.53) trial types (**Supplemental Figure 4**). RT exhibited a significant
425 interaction effect for both congruent (F[1, 111.2] = 6.24, p = 0.01) and incongruent (F[1, 110.95]
426 = 6.25, p = 0.01) trial types. *Post-hoc* comparisons indicated no baseline differences between
427 treatments for RT (all FDR p > 0.30). At endpoint, RT was faster following SCF in both congruent
428 (β = -9.65, SE = 3.92, 95% CI: [-17.43, -1.88], FDR p = 0.01) and incongruent (β = -14.2, SE =
429 4.68, 95% CI: [-23.49, -4.95], FDR p = 0.003) trials (**Figure 3**).
430 P3 distribution was visualized (**Supplemental Figure 5**).No interaction was observed for
431 P3 amplitude during congruent (F[1, 100.76] = 0.56, p = 0.46) or incongruent (F[1, 99.33] = 0.96,
432 p = 0.33) trial type, nor for peak latency during congruent (F[1, 98.69] = 0.23, p = 0.63) or
433 incongruent (F[1, 98.87] = 2.26, p = 0.14) trial types. No treatment-by-time interaction effect was
434 detected for ACC (β = -1.32, SE = 0.80, 95% CI: [-2.87, 0.24], p = 0.10) or RT (β = -2.69, SE =
435 3.12, 95% CI: [-8.78, 3.40], p = 0.39) interference scores.
436
437 *Mood and Stress*
438 No treatment-by-time effects were observed for any secondary outcomes. Mood subscales
439 and total mood disturbance (*POMS*; all p > 0.53), relational memory performance (*iPosition*; all p

440 > 0.45), affect (*PANAS*; all $p > 0.45$), and stress (*PSS*-10; $p = 0.70$), showed no differences
441 (**Supplemental Table 1**). Similarly, no effects were observed across *CANTAB* measures (all $p >$
442 0.13) (**Supplemental Table 2-5**).
443
444 **Aim 2: Gut Microbiota and Metabolite Outcomes**
445 *16S Fecal microbiota*
446 Alpha diversity showed an interaction effect with observed richness (F[1, 108.0] = 6.69,
447 FDR $p = 0.03$), with marginal effects for Faith's PD (F[1, 108.14] = 3.63, FDR $p = 0.09$) and none
448 with Shannon (FDR $p = 0.26$). *Post-hoc* indicated no baseline difference in richness ($\beta = -1.04$, SE
449 = 8.69, 95% CI: [-16.5, 18.5], FDR $p = 0.91$) and was reduced following SCF at endpoint ($\beta = -$
450 29.86, SE = 8.55, 95% CI [-47.1, -12.6], FDR $p = 0.01$) (**Table 5**; **Supplemental Figure 6)**. Beta
451 diversity showed a small but statistically significant interaction across Bray-Curtis (F = 0.81, ΔR^2
452 = 0.005, FDR $p < 0.001$), Unweighted Uni-Frac (F = 0.47, $\Delta R^2 = 0.003$, FDR $p = 0.002$), and
453 Weighted Uni-Frac (F = 1.07, $\Delta R^2 = 0.007$, FDR $p < 0.001$) (**Supplemental Figure 7)**. *Post-hoc*
454 comparisons for each metric showed differences with SCF relative to its baseline (Bray-Curtis: F
455 = 1.37, $\Delta R^2 = 0.019$, FDR $p < 0.001$; Unweighted: F = 0.43, $\Delta R^2 = 0.006$, FDR $p = 0.03$; Weighted:
456 F = 1.69, $\Delta R^2 = 0.023$, FDR $p < 0.001$) and at endpoint relative to CON (Bray-Curtis: F = 1.39,
457 $\Delta R^2 = 0.019$, FDR $p < 0.001$, Unweighted: F = 0.64, $\Delta R^2 = 0.010$, FDR $p = 0.005$; Weighted: F =
458 1.69, $\Delta R^2 = 0.023$, FDR $p < 0.001$). No differences were observed between baseline periods and
459 during the CON intervention (all FDR $p > 0.85$).
460 At the phylum level, none met the significance threshold (**Supplemental Table 6**). A total
461 of 260 genera were detected, 128 passed the filtering criteria (≥40% prevalence, >10 reads), and
462 14 met the significance threshold (FDR $p < 0.05$); 11 were classified as low-abundance taxa

463 (<0.5%) or incertae_sedis (**Supplemental Table 7)**. *Parabacteroides* enrichment was consistently
464 observed across 90% of participants (**Figure 4**), demonstrating an interaction effect (χ^2 = 42.0,
465 FDR p < 0.001)**.** *Post-hoc* indicated no baseline differences for *Parabacteroides* between
466 treatments (β = 0.02, SE = 0.16, 95% CI [-0.29, 0.33], FDR p = 0.91) and was enriched ~4.1-log
467 fold by endpoint following SCF compared to CON (β = -1.42, SE = 0.16, 95% CI [-1.74, -1.11],
468 FDR p < 0.001). *Fusicatenibacter* had an interaction (χ^2 = 17.94, FDR p < 0.001), no baseline
469 differences (β = 0.14, SE: 0.19, 95% CI: [-0.23, 0.50], FDR p = 0.64), and ~2.7-log fold enrichment
470 following SCF (β = -0.97, SE: 0.18, 95% CI: [-1.34, -0.60], FDR P<0.001). Similarly, *Dialister*
471 had an interaction (χ^2 = 7.25, FDR p = 0.02), no baseline differences (β = 0.17, SE: 0.26, 95% CI:
472 [-0.33, 0.68], FDR p = 0.50), and ~2.4-log fold enrichment following SCF (β = -0.89, SE: 0.30,
473 95% CI: [-1.48, -0.30], FDR p = 0.03) (**Figure 4**).
474
475 *Microbial metabolites*
476 Fecal SCFAs (**Supplemental Figure 8**) and BCFAs did not statistically differ between
477 treatments (all p > 0.14; **Table 4**). Pooled total indoles (indole, 2-methylindole, 3-methylindole,
478 7-methylindole), indole, pooled total phenols (4-methylphenol, 4-ethylphenol, phenol), 4-
479 methylindole, and ammonia likewise did not show an interaction effect (all p > 0.32;
480 **Supplemental Table 8**).
481
482 *Gastrointestinal symptoms*
483 Symptom severity scores were generally absent to mild across conditions. No differences
484 were observed between treatments for changes in cramping, nausea, reflux, rumbling, or burping
485 (all p > 0.17; **Table 5**). Flatulence severity was scored increased following SCF (p = 0.01), while

486 bloating was marginally increased following SCF (p = 0.05). No interaction effect was observed
487 for self-reported consistency, ease of passage, bowel frequency, or fecal pH (all p > 0.22;
488 **Supplemental Table 9**).
489
490 **Aim 3: Integrative and Functional Analyses**
491 *Correlation analyses*
492 Spearman correlations were used to examine associations between selected microbial and
493 metabolite candidates (acetate, propionate, *Parabacteroides*, *Fusicatenibacter*, *Dialister*) and
494 flanker RT (**Figure 5**). For congruent trials, RT showed marginal inverse associations with acetate
495 (ρ = -0.33, FDR p = 0.09) and propionate (ρ = -0.36, FDR p = 0.09). *Parabacteroides* was
496 marginally associated with acetate (ρ = 0.34, FDR p = 0.09). No genera were associated with
497 congruent RT (all FDR p > 0.14). For incongruent trials, no significant correlation was detected
498 for any candidate (all ρ < 0.23 and FDR p > 0.30) **(Supplementary Figure 9)**.
499
500 *Mediation analyses*
501 Causal mediation models tested whether microbial and metabolite candidates mediated the
502 treatment effect on RT. For congruent trials, no candidate showed a significant indirect effect, with
503 proportion of the treatment effected mediated estimated less than 10.0% across all. For incongruent
504 trials, mediation similarly demonstrated null mediation effects with proportions estimated less than
505 4.1% (**Table 6**). For both congruencies, sensitivity analyses indicated that weak correlations
506 between mediator and outcome error terms (ρ = -0.1) reduces the mediation effect to zero.
507
508 *Moderation analyses*

509 Moderation models tested whether changes in microbial and metabolite candidates
510 moderated the strength of the SCF-effect on RT. No interaction was observed across candidate
511 moderators (all RT $p > 0.49$) except for *Parabacteroides*, showing a moderation effect with
512 congruent ($p = 0.05$) and incongruent RTs ($p = 0.04$). Adding *Parabacteroides* to the model
513 increased explained variance from $\Delta R^2 = 0.07$ (base model) to $\Delta R^2 = 0.12$ (adjusted), whereas
514 other markers contributed less than 1% (**Table 7**).

515 *Post-hoc* simple slopes provided further resolution of the moderation effect from
516 *Parabacteroides*. For congruent trials, SCF treatment was associated with faster RT when
517 *Parabacteroides* changes were small (-1SD: $\beta = -29.51$, SE = 8.76, $t = -3.37$, 95% CI: [-47.0, -
518 12.03], $p < 0.001$), but not when *Parabacteroides* change was near the mean (0 SD; $\beta = -9.74$, SE
519 = 8.27, $t = -1.18$, 95% CI: [-26.2, 6.76], $p = 0.24$) or when increases were much larger (+1 SD: β
520 = 10.03, SE = 16.27, $t = 0.62$, 95% CI: [-22.5, 42.51], $p = 0.54$).

521 For incongruent trials, the same pattern emerged, SCF was associated with faster RTs at
522 smaller *Parabacteroides* increases ($\beta = -32.36$, SE = 10.59, $t = -3.06$, 95% CI: [-53.5, -11.2], $p <$
523 0.001), but not at the mean ($\beta = -7.30$, SE = 10.0, $t = -0.73$, 95% CI: [-27.3, 12.7], $p = 0.47$) or
524 larger enrichments ($\beta = 17.75$, SE = 19.68, $t = -0.90$, 95% CI: [-21.5, 57.0], $p = 0.37$) (**Figure 7**).
525

526 *In vitro culturing of P. distasonis*

527 *P. distasonis* was confirmed to grow with SCF in isolation displaying a distinct growth
528 kinetics with significant media effect ($F[2,42] = 9.39$, $p < 0.001$), time ($F[6,42] = 239.6$, $p < 0.001$),
529 and interaction ($F[12,4] = 32.7$, $p < 0.001$). Growth on glucose and CON showed a short lag phase
530 (<1h), and a rapid log phase reaching stationary phase within 5-6h (glucose: $OD_{600} = 0.59$, 5.5h;
531 CON: $OD_{600} = 0.54$, 5h). Growth on SCF exhibited a two-phase diauxic growth pattern: a slower

532 and smaller initial phase reaching OD_{600} = 0.31 at 6h, followed by a ~2h lag, then a second log
533 phase that peaked at OD_{600} = 0.61 by 14h. *Post-hoc* comparisons showed that SCF had
534 significantly lower growth rates at 2h (all FDR $p < 0.001$) and 4h (vs. glucose, FDR $p = 0.03$; vs.
535 CON, FDR $p = 0.01$) relative to controls. By 6h, no differences were detected across treatments.
536 At 8-10h, SCF had higher growth rates compared to controls (all FDR $p < 0.001$), and remained
537 higher at 12h (vs. glucose, FDR $p = 0.002$). By 14h, growth stabilized with no differences detected
538 between treatments (**Figure 8)**.
539
540 *Predictive functional metagenomic analyses*
541 Unstratified KEGG Orthology (KO) analysis detected *N*-glycan biosynthesis and α-
542 linolenic acid metabolism pathways significantly enriched following SCF at endpoint (all FDR p
543 < 0.01). Unstratified EC (enzyme commission) analysis detected 23 enzyme functions that differed
544 between treatments (all FDR $p < 0.05$) (**Supplemental Figure 10**). Significant pairwise
545 differences were observed only for SCF compared with its baseline and CON at endpoint.
546 MaAsLin2 detected 2,701 carbohydrate-metabolism KOs associated with SCF at endpoint (FDR
547 $p < 0.05$). Pairwise comparisons showed significant differences in 1,778 KOs during the SCF
548 intervention, 4 during CON intervention, and none between baselines. Among the top SCF-
549 associated KOs, 18 showed contribution from *Parabacteroides* including glycan degradation and
550 complex carbohydrate utilization and two from *Fusicatenibacter* (**Supplemental Figure 11**).
551
552 *Responder shotgun metagenomics analyses*
553 Shotgun genus-level profiles confirmed that *Parabacteroides* increased in responders (Δ =
554 13.6%) and slightly decreased in non-responders (Δ = -0.4%), consistent with 16S results. At the

555 species level, *P. distasonis* increased in responders (Δ = 10.9%) and remained undetectable in non-
556 responders, while *P. merdae* also increased in responders (Δ = 2.7%) and decreased in non-
557 responders (Δ = -0.4%). *F. saccharivorans* negligibly increased in responders (Δ = 0.1%),
558 compared to a larger increase in non-responders (Δ = 2.2%). *D. hominis* (Δ = 1.4%) and *D. invisus*
559 (0.3%) increased in non-responder, while only *D. invisus* was detected and decreased in responders
560 (Δ = -0.3%). Ordination by responder type were also observed using Bray-Curtis and Jaccard
561 indices (**Supplemental Figure 12)**.

562 Functional analyses with *HUMAnN* showed an increase in carbohydrate metabolism-
563 related KOs among responders (UDP-glucose 6-dehydrogenase, α-amylases, hexokinase), while
564 non-responders demonstrated a lack of presence in these KOs (**Figure 9**). Genus- (**Supplemental**
565 **Figure 13)** and species-level time comparisons (**Figure 10**) in responders showed increased
566 contributions from *P. distasonis* to multiple carbohydrate-active gene families, including glycoside
567 hydrolases (GHs), α-amylases, and hexokinase. Analyses using CAZy annotations to provide
568 further resolution of GH families and subfamilies between groups. Of 228 GH families detected,
569 those with positive log fold changes in responders were isolated (**Supplemental Figure 14**).
570 Several GH families were enriched (GH43_8, GH43_33, GH25, GH24, GH179, GH13_9,
571 GH130_2, GH12) and showed positive spearman rho values with *Parabacteroides* abundances
572 (**Supplemental Figure 15**).

573 Microbial responders demonstrated faster RT across the SCF intervention for both
574 congruent (Δ = -0.90ms) and incongruent (Δ = 2.7ms) trials. In contrast, non-responders exhibited
575 slower baseline RT but demonstrated larger SCF-induced improvements (congruent Δ = -32.1ms,
576 incongruent Δ = -31.8ms). Parallel changes were observed in SCFAs; responders had higher
577 baseline SCFA levels and was increased in both groups for acetate (responders Δ = 66.4 vs. non-

578 responders Δ = 71.6 µmol/g DMB) and propionate (responders Δ = 20.9 vs. non-responders Δ =
579 28.6 µmol/g µmol/g DMB). (**Table 8**).
580
581 **Discussion**
582 In this randomized crossover trial, SCF improved attentional inhibition, reflected by faster
583 RT without compromising accuracy on both congruent and incongruent flanker task trial types.
584 Effects were domain-specific to attentional inhibition, with no changes in relational memory, rule
585 acquisition and reversal, set shifting, sustained attention, response inhibition, or spatial working
586 memory observed (*Aim 1*). SCF also shifted fecal microbial diversity, selectively enriching
587 *Parabacteroides*, numerically increasing fecal acetate, and yielded mild GI symptoms, consistent
588 with its role as a fermentable and generally well tolerated fiber (*Aim 2*). Further, SCF had no effect
589 on P3 amplitude or latency, mood, or stress. Exploratory analyses did not identify any mediators
590 but suggested that *Parabacteroides* may conditionally influence SCF-related RT improvements.
591 Shotgun metagenomics identified *P. distasonis* as the primary responsive, while *in vitro* culturing
592 independently confirmed its capacity to metabolize SCF independent of cross-feeding (*Aim 3*).
593 Attentional inhibition is a core domain of cognitive control that can naturally and
594 insidiously decline with aging [31], underscoring the need for dietary strategies to preserve healthy
595 cognitive aging. Few clinical trials have assessed the impact of dietary fiber on cognition while
596 integrating microbiome outcomes. Here, SCF selectively supported attentional inhibition, reflected
597 by faster RT in congruent and incongruent flanker trials, with no changes in other cognitive
598 outcomes. This domain-specific pattern reinforces the concept that gut-brain communication can
599 influence higher-order cognitive processes. Another randomized trial among 84 adults with
600 overweight and obesity observed greater accuracy, but not RT, during a modified flanker task
601 following 12 weeks of daily avocado consumption (12.8-16 grams fiber) relative to a control

602 providing 3.2 – 4 grams fiber daily [92]. Additional analyses showed an increase in α-diversity and
603 enriched *Faecalibacterium, Lachnospira*, and *Alistipes* and 18% greater fecal acetate, 70%
604 greater stearic acid, and 98% greater palmitic acid concentrations due to fiber-rich avocado
605 consumption, however, no mediation or moderation analyses were conducted [93]. Another nutrition
606 trial reported mood benefits with 16 g inulin/day for 12 weeks versus 16 g maltodextrin among
607 adults with obesity, particularly among individuals exhibiting a specific microbial signature,
608 however, no effects were observed on inhibitory control, working memory, or cognitive flexibility
609 regardless of changes in the gut microbiota [39]. Other lifestyle interventions, such as increased
610 physical activity, have been shown to improve flanker RT acutely, with one randomized trial
611 among 106 healthy-weight adults showing improvements in both congruent (458 ms vs 475 ms)
612 and incongruent (528 ms vs 547 ms) paradigms following 30 min of high-intensity aerobic exercise
613 compared with seated rest [94]. Together, these studies suggest that cognition effects are domain-
614 and context-specific, shaped by factors such as fiber type, population characteristics, physical
615 activity status, and intervention duration, which complicates direct cross-study comparisons but
616 underscores nutrition as a potential modifiable factor for cognitive health.

617 Consistent with previous SCF trials, *Parabacteroides* was enriched following the
618 intervention [21,95,96]. The convergence of 16S and shotgun metagenomes strengthens the confidence
619 that this enrichment reflects a biological response rather than a methods artifact. In responders, *P.*
620 *distasonis* abundance was inversely related to *Bacteroides vulgatus*, suggesting possible ecological
621 competition under SCF exposure. Predictive and shotgun metagenomics indicated increased
622 carbohydrate metabolism pathways and glycan degradation capacity, with CAZy highlighting the
623 enrichment of *Parabacteroides*-linked GHs (GH35, GH43, and GH73) [97,98]. *P. distasonis*-specific
624 GHs (GH144 and GH13) involved in the hydrolysis α-glycosidic bonds were also detected [97,98].

625 CAZymes serving similar functions are typically organized within PULs, gene clusters that
626 coordinate sensing, import, and degradation of dietary glycans [99]. The enrichment of these
627 CAZymes likely reflects an activation of SCF-targeting PULs, enabling *P. distasonis* to maintain
628 a competitive niche in the large intestine. Our *in vitro* experiment supported this metabolic
629 capacity, showing that *P. distasonis*, with no prior SCF exposure, fermented SCF in a diauxic
630 pattern, consistent with the mixture of fiber and non-fiber starches in the formula. Together, these
631 findings position *Parabacteroides* as a primary degrader of SCF, although mechanistic insights
632 remain limited.

633 These findings are consistent with the ISAPP definition of a prebiotic: "a substrate that is
634 selectively utilized by host microorganisms, conferring a health benefit" [100]. SCF met these criteria
635 by inducing a small shift in the GI microbiota, selective utilization by *Parabacteroides*, and
636 conferring a cognitive benefit in healthy older adults. *Parabacteroides* responded to SCF in 90%
637 of the healthy cohort, consistent with the 'Health-Associated Core Keystone' (HACK) index [101],
638 which identified *P. distasonis, P. merdae*, and *F. saccharivorans* as core and stability-associated
639 taxa [78]. Prior work links *P. distasonis* with anti-inflammatory effects, gut barrier protection [102–104],
640 and neuroactive metabolite production (e.g., GABA) [105], all processes relevant to gut-brain
641 communication. Although *Parabacteroides* did not directly mediate cognitive benefits in this
642 study, its consistent response to SCF highlights its role as a keystone taxon in healthy older adults
643 [97,102–104,106,107].

644 In this study, fecal SCFAs did not reach statistical significance, however, their directional
645 changes align with prior dietary fiber interventions and remain plausible candidates for gut-brain
646 signaling given their ability to cross and modulate the blood-brain barrier's structural integrity
647 [34,35,108–111]. Prior human studies show that colonic SCFA delivery influences anticipatory brain

648 reward responses and attenuates cortisol reactivity to psychosocial stress [35]. Despite biological
649 plausibility, in this study, mediation and moderation models did not support fecal SCFAs as either
650 mediators or moderators of the SCF effect. However, moderation analyses did suggest that the
651 SCF effect on RT may have depended on the magnitude of change in *Parabacteroides*. Greater
652 RT improvements were observed when *Parabacteroides* increases were small to modest, whereas
653 larger increases were not associated with faster RTs. Furthermore, microbial responders
654 consistently performed quicker at baseline and endpoints, while non-responders exhibited larger
655 improvements from SCF for RT speeds. These exploratory findings suggest that *Parabacteroides*
656 may exert a context-dependent influence, but its enrichment may not be linearly beneficial for
657 cognitive performance.

658 Secondary taxa provided additional exploratory context. *Dialister* was the only genus to
659 suggest a potential adverse mediation effect, whereas *Fusicatenibacter* showed the largest
660 proportion mediated. Bacillota members (e.g., *Fusicatenibacter*) are capable of cross-feeding on
661 substrates released by members of the Bacteroidota phylum [112] (e.g., *Parabacteroides*), producing
662 beneficial metabolites including acetate, lactate, formate, and succinate [113]. Potentially,
663 *Fusicatenibacter* may have had the role of the main secondary consumer working with
664 *Parabacteroides* in response to SCF. Microbial responders had higher baseline levels of *F.*
665 *saccharivorans* and showed negligible enrichment with SCF, whereas non-responders exhibited a
666 relatively larger enrichment. In contrast, *D. invisus* and *D. hominis* were enriched only in non-
667 responders and remained below detectable levels in responders. A prior study linked
668 *Fusicatenibacter saccharivorans* with executive and visuospatial functions with community-
669 dwelling older adults [114], whereas *Dialister invisus* was found more abundant in older adults with
670 mild cognitive impairment [114]. These patterns suggests that baseline microbial composition and

671 differential responsiveness may contribute to cognitive variability, though mechanistic inferences
672 remain preliminary.

673 The study has several limitations. First, the cohort was predominantly white, female, and
674 highly educated, which may restrict generalizability. Mediation and moderation analysis were
675 exploratory and did not fully account for the crossover design in its statistical framework and
676 utilized change and baseline adjustments. Shotgun metagenomics was limited to a small subset of
677 responders and non-responders, reducing power to detect subtle effects. The absence of systemic
678 samples prevent assessment of circulating SCFAs or other metabolites, while the targeted
679 metabolomics panel may have overlooked additional relevant compounds (e.g., tryptophan
680 catabolites). Although participants agreed to maintain their habitual diets, inter-individual dietary
681 variation may have introduced unmeasured noise into microbiome and metabolite outcomes.
682 Despite these limitations, the study provides novel evidence linking SCF to selective cognitive
683 benefits, supported by exploratory insights into microbial and SCFA response.

684 In conclusion, four weeks SCF improved RT in middle aged and older adults and induced
685 a small microbiota shift dominated by *Parabacteroides*. Exploratory moderation suggested a
686 threshold effect, with RT benefits most evident at smaller changes in *Parabacteroides*. Notably,
687 cognitive improvements were also observed in non-responders with negligible *Parabacteroides*,
688 indicating that cognitive benefits are unlikely to hinge on a single taxon but may instead depend
689 on the ecological context and balance between health associated keystone microbes (e.g.,
690 *Parabacteroides* and *Fusicatenibacter*) for contributing complementary routes to induce GI-brain
691 interactions [115]. These findings position SCF as a dietary fiber with potential cognitive relevance,
692 while underscoring the need for multi-omics, untargeted metabolomics, dosing trials, and systemic

biomarker assessments to refine mechanistic models and advance precision nutrition strategies for cognitive health.

Acknowledgments

We thank Dr. Michael J. Miller for his expertise, equipment, and facility to conduct the *in vitro* culturing experiment. We also thank Dr. Pratik Banerjee and his graduate students (Papri Suraya Rahman and Edwin Valenzuela De Leon) for providing the *P. distasonis* strain and assisting with the equipment set-up. We are also grateful to the HDH graduate students: Alexis Baldeon, Marahi Perez-Tamayo, Nadine Veasely, and Maria Sanabria-Veaz; HDH staff: Eva Cornman, Myra Esmail, Karen Gutierrez, and Tehila Abdiel; and NAK graduate students Shelby Keyes and John Kim, as well as the undergraduate research assistants from HDH and NAK laboratories, for their assistance during the appointments, sample processing, and data management.

Author Contributions

HDH, NAK, DAA and TAH: designed the research; MDB and TM: recruited and enrolled participants and coordinated study procedures; DAA: conducted the *in vitro* experiment; DAA, TAH, SM, TM and RS: conducted the experiments and testing appointments; MA, DR and DAA: managed biological samples collection and storages; DAA and TAH: managed study data; DAA and NS: prepared data for bioinformatic pipelines; DAA and TAH: analyzed the data: DAA, TAH, NAK and HDH: wrote the manuscript; NAK and HDH: had primary responsibility for final content. All authors read and approved the final manuscript.

Author Disclosures: The authors report no conflict of interest.

Funding: This work was supported by Tate & Lyle Ingredients Americas LLC and the USDA NIFA, Hatch Project (1026591, to HDH).

Data Availability: Data described in the manuscript, code book, and analytic code will be made available upon request.

721 **References**
722

723 1. Morris MC, Wang Y, Barnes LL, Bennett DA, Dawson-Hughes B, Booth SL. Nutrients
724 and bioactives in green leafy vegetables and cognitive decline: Prospective study.
725 *Neurology*. 2018;90(3):E214-E222. doi:10.1212/WNL.0000000000004815
726 2. Perim Baldo M, Aboussaleh Y, Turrini A, et al. Adherence to a Mediterranean-Style Diet
727 and effects on Cognition in Adults: A Qualitative evaluation and Systematic Review of
728 Longitudinal and Prospective Trials. 2016;3:1. doi:10.3389/fnut.2016.00022
729 3. Khan NA, Raine LB, Donovan SM, Hillman CH. IV. The cognitive implications of
730 obesity and nutrition in childhood. *Monogr Soc Res Child Dev*. 2014;79(4):51-71.
731 doi:10.1111/mono.12130
732 4. Cho SS, Qi L, Fahey GC, Klurfeld DM. Consumption of cereal fiber, mixtures of whole
733 grains and bran, and whole grains and risk reduction in type 2 diabetes, obesity, and
734 cardiovascular disease. *American Journal of Clinical Nutrition*. 2013;98(2):594-619.
735 doi:10.3945/ajcn.113.067629
736 5. Trock B, Lanza E, Greenwald P, Lanza E, Greenwald P. *REVIEW Dietary Fiber,*
737 *Vegetables, and Colon Cancer: Critical Review and Meta-Analyses of the Epidemiologic*
738 *Evidence*. https://academic.oup.com/jnci/article/82/8/650/882222
739 6. Gov D. *Dietary Guidelines for Americans Make Every Bite Count With the Dietary*
740 *Guidelines*. https://www.
741 7. Marchesi JR, Ravel J. The vocabulary of microbiome research: a proposal. *Microbiome*.
742 2015;3(1). doi:10.1186/s40168-015-0094-5
743 8. Fleming SA, Monaikul S, Patsavas AJ, Waworuntu R V., Berg BM, Dilger RN. Dietary
744 polydextrose and galactooligosaccharide increase exploratory behavior, improve
745 recognition memory, and alter neurochemistry in the young pig. *Nutr Neurosci*.
746 2019;22(7):499-512. doi:10.1080/1028415X.2017.1415280
747 9. Gronier B, Savignac HM, Miceli M Di, et al. Increased cortical neuronal responses to
748 NMDA and improved attentional set-shifting performance in rats following prebiotic (B-
749 GOS s) ingestion. doi:10.1016/j.euroneuro.2017.11.001
750 10. Khan NA, Raine LB, Drollette ES, Scudder MR, Kramer AF, Hillman CH. Dietary Fiber
751 Is Positively Associated with Cognitive Control among Prepubertal Children. *J Nutr*.
752 2015;145(1):143-149. doi:10.3945/JN.114.198457
753 11. Hassevoort KM, Lin AS, Khan NA, Hillman CH, Cohen NJ. Added sugar and dietary
754 fiber consumption are associated with creativity in preadolescent children. *Nutr Neurosci*.
755 2020;23(10):791-802. doi:10.1080/1028415X.2018.1558003
756 12. Naveed S, Venäläinen T, Eloranta AM, et al. Associations of dietary carbohydrate and
757 fatty acid intakes with cognition among children. *Public Health Nutr*. 2020;23(9):1657-
758 1663. doi:10.1017/S1368980019003860
759 13. Cryan JF, O KJ, M Cowan CS, et al. The Microbiota-Gut-Brain Axis. *Physiol Rev*.
760 2019;99:1877-2013. doi:10.1152/physrev.00018.2018.-The
761 14. Stewart ML, Nikhanj SD, Timm DA, Thomas W, Slavin JL. Evaluation of the effect of
762 four fibers on laxation, gastrointestinal tolerance and serum markers in healthy humans.
763 *Ann Nutr Metab*. 2010;56(2):91-98. doi:10.1159/000275962
764 15. Shuan W, Tan K, Fen P, et al. The Role of Soluble Corn Fiber on Glycemic and Insulin
765 Response. doi:10.3390/nu12040961

16. Jakeman SA, Henry CN, Martin BR, et al. Soluble corn fiber increases bone calcium retention in postmenopausal women in a dose-dependent manner: A randomized crossover trial. *American Journal of Clinical Nutrition*. 2016;104(3):837-843. doi:10.3945/ajcn.116.132761
17. Klosterbuer AS, Hullar MAJ, Li F, et al. Gastrointestinal effects of resistant starch, soluble maize fibre and pullulan in healthy adults. doi:10.1017/S0007114513000019
18. LinAmy AHM, Nichols BL, Quezada-Calvillo R, et al. Unexpected high digestion rate of cooked starch by the Ct-maltase-glucoamylase small intestine mucosal α-glucosidase subunit. *PLoS One*. 2012;7(5). doi:10.1371/journal.pone.0035473
19. Vester Boler BM, Rossoni Serao MC, Bauer LL, et al. Digestive physiological outcomes related to polydextrose and soluble maize fibre consumption by healthy adult men. *British Journal of Nutrition*. 2011;106(12):1864-1871. doi:10.1017/S0007114511002388
20. Maathuis A, Venema K, Hoffman A, Evans A, Sanders L. The effect of the undigested fraction of maize products on the activity and composition of the microbiota determined in a dynamic in vitro model of the human proximal large intestine. *J Am Coll Nutr*. 2009;28(6):657-666. doi:10.1080/07315724.2009.10719798
21. Whisner CM, Martin BR, Nakatsu CH, et al. Soluble corn fiber increases calcium absorption associated with shifts in the gut microbiome: A randomized dose-response trial in free-living pubertal females. *Journal of Nutrition*. 2016;146(7):1298-1306. doi:10.3945/jn.115.227256
22. Arroyo MC, Laurie I, Rotsaert C, Marzorati M, Risso D, Karnik K. Age-Dependent Prebiotic Effects of Soluble Corn Fiber in M-SHIME® Gut Microbial Ecosystems. *Plant Foods for Human Nutrition*. 2023;78(1):213-220. doi:10.1007/s11130-023-01043-z
23. Holscher HD, Gregory Caporaso J, Hooda S, Brulc JM, Fahey GC, Swanson KS. Fiber supplementation influences phylogenetic structure and functional capacity of the human intestinal microbiome: Follow-up of a randomized controlled trial. *American Journal of Clinical Nutrition*. 2015;101(1):55-64. doi:10.3945/ajcn.114.092064
24. Brown AJ, Goldsworthy SM, Barnes AA, et al. The orphan G protein-coupled receptors GPR41 and GPR43 are activated by propionate and other short chain carboxylic acids. *Journal of Biological Chemistry*. 2003;278(13):11312-11319. doi:10.1074/jbc.M211609200
25. Cani PD, Lecourt E, Dewulf EM, et al. Gut microbiota fermentation of prebiotics increases satietogenic and incretin gut peptide production with consequences for appetite sensation and glucose response after a meal. *American Journal of Clinical Nutrition*. 2009;90(5):1236-1243. doi:10.3945/ajcn.2009.28095
26. Corrêa-Oliveira R, Fachi JL, Vieira A, Sato FT, Vinolo MAR. Regulation of immune cell function by short-chain fatty acids. *Clin Transl Immunology.John Wiley and Sons Inc.* 2016;5(4). doi:10.1038/cti.2016.17
27. Dalile B, Van Oudenhove L, Vervliet B, Verbeke K. The role of short-chain fatty acids in microbiota–gut–brain communication. *Nat Rev Gastroenterol Hepatol.Nature Publishing Group*. 2019;16(8):461-478. doi:10.1038/s41575-019-0157-3
28. Zhou SY, Guo ZN, Yang Y, Qu Y, Jin H. Gut-brain axis: Mechanisms and potential therapeutic strategies for ischemic stroke through immune functions. *Front Neurosci.Frontiers Media S.A.* 2023;17. doi:10.3389/fnins.2023.1081347

29. Silva YP, Bernardi A, Frozza RL. The Role of Short-Chain Fatty Acids From Gut Microbiota in Gut-Brain Communication. *Front Endocrinol (Lausanne).Frontiers Media S.A.* 2020;11. doi:10.3389/fendo.2020.00025
30. Mansuy-Aubert V, Ravussin Y. Short chain fatty acids: the messengers from down below. *Front Neurosci*. 2023;17. doi:10.3389/fnins.2023.1197759
31. Diamond A. Executive functions. *Annu Rev Psychol.Annual Reviews Inc.* 2013;64:135-168. doi:10.1146/annurev-psych-113011-143750
32. Duncan-Johnson CC. P300 latency: A new metric of information processing. *Psychophysiology*. 1981;18(3):207-215. doi:10.1111/j.1469-8986.1981.tb03020.x
33. Polich J. Updating P300: An integrative theory of P3a and P3b. *Clinical Neurophysiology*. 2007;118(10):2128-2148. doi:10.1016/j.clinph.2007.04.019
34. La Torre D, Verbeke K, Dalile B. Dietary fibre and the gut–brain axis: microbiota-dependent and independent mechanisms of action. *Gut Microbiome*. 2021;2. doi:10.1017/gmb.2021.3
35. Dalile B, Fuchs A, La Torre D, Vervliet B, Van Oudenhove L, Verbeke K. Colonic butyrate administration modulates fear memory but not the acute stress response in men: A randomized, triple-blind, placebo-controlled trial. *Prog Neuropsychopharmacol Biol Psychiatry*. 2024;131. doi:10.1016/j.pnpbp.2024.110939
36. Cheng J, Hu H, Ju Y, et al. Gut microbiota-derived short-chain fatty acids and depression: deep insight into biological mechanisms and potential applications. *Gen Psychiatr.BMJ Publishing Group*. 2024;37(1). doi:10.1136/gpsych-2023-101374
37. Luqman A, He M, Hassan A, et al. Mood and microbes: a comprehensive review of intestinal microbiota's impact on depression. *Front Psychiatry.Frontiers Media SA*. 2024;15. doi:10.3389/fpsyt.2024.1295766
38. Haskell CF, Scholey AB, Jackson PA, et al. Cognitive and mood effects in healthy children during 12 weeks' supplementation with multi-vitamin/minerals. *British Journal of Nutrition*. 2008;100(5):1086-1096. doi:10.1017/S0007114508959213
39. Leyrolle Q, Cserjesi R, D.G.H. Mulders M, et al. Prebiotic effect on mood in obese patients is determined by the initial gut microbiota composition: A randomized, controlled trial. *Brain Behav Immun*. 2021;94:289-298. doi:10.1016/j.bbi.2021.01.014
40. Godin-Leisure-Time-Exercise-Questionnaire_070815.
41. Edwards CG, Walk AM, Cannavale CN, et al. Dietary choline is related to neural efficiency during a selective attention task among middle-aged adults with overweight and obesity. *https://doi.org/101080/1028415X20191623456*. 2019;24(4):269-278. doi:10.1080/1028415X.2019.1623456
42. Chatrian GE, Lettich E, Nelson PL. American Journal of EEG Technology Ten Percent Electrode System for Topographic Studies of Spontaneous and Evoked EEG Activities Ten Percent Electrode System for Topographic Studies of Spontaneous and Evoked EEG Activities. Published online 2015. doi:10.1080/00029238.1985.11080163
43. Delorme A, Makeig S. EEGLAB: An open source toolbox for analysis of single-trial EEG dynamics including independent component analysis. *J Neurosci Methods*. 2004;134(1):9-21. doi:10.1016/J.JNEUMETH.2003.10.009
44. Lopez-Calderon J, Luck SJ. ERPLAB: An open-source toolbox for the analysis of event-related potentials. *Front Hum Neurosci*. 2014;8(1 APR):213. doi:10.3389/FNHUM.2014.00213/BIBTEX

45. Kamijo K, Pontifex MB, Khan NA, et al. The association of childhood obesity to neuroelectric indices of inhibition. *Psychophysiology*. 2012;49(10):1361-1371. doi:10.1111/J.1469-8986.2012.01459.X
46. Walk AM, Edwards CG, Baumgartner NW, et al. The role of retinal carotenoids and age on neuroelectric indices of attentional control among early to middle-aged adults. *Front Aging Neurosci*. 2017;9(JUN):183. doi:10.3389/FNAGI.2017.00183/BIBTEX
47. Luck SJ, Gaspelin N. How to get statistically significant effects in any ERP experiment (and why you shouldn't). *Psychophysiology*. 2017;54(1):146-157. doi:10.1111/PSYP.12639
48. Pontifex MB. Stylized Topographic Map Plugin for EEGLAB/ERPLAB.
49. Horecka KM, Dulas MR, Schwarb H, Lucas HD, Duff M, Cohen NJ. Reconstructing relational information. *Hippocampus*. 2018;28(2):164-177. doi:10.1002/hipo.22819
50. Langley C, Sahakian B, Robbins T. Cambridge neuropsychological test automated battery (cantab). *SAGE Publications Ltd*. 2023;0:435-468.
51. Wild K V., Musser ED. The cambridge neuropsychological test automated battery in the assessment of executive functioning. In: *Handbook of Executive Functioning*. Springer New York; 2014:171-190. doi:10.1007/978-1-4614-8106-5_11
52. Stephen J. Gibson. The Measurement of Mood States in Older Adults. *The Journals of Gerontology: Series B*. 1997;52B(4):167-174.
53. Boyle GJ, Helmes E, Matthews G, Izard CE. Measures of Affect Dimensions. In: *Measures of Personality and Social Psychological Constructs*. Elsevier Inc.; 2015:190-224. doi:10.1016/B978-0-12-386915-9.00008-5
54. Humboldt S von, Monteiro A, Leal I. Validation of the PANAS: A Measure of Positive and Negative Affect for Use with Cross-National Older Adults. *Rev Eur Stud*. 2017;9(2):10. doi:10.5539/res.v9n2p10
55. Lee EH. Review of the psychometric evidence of the perceived stress scale. *Asian Nurs Res (Korean Soc Nurs Sci)*. 2012;6(4):121-127. doi:10.1016/j.anr.2012.08.004
56. Callahan BJ, McMurdie PJ, Rosen MJ, Han AW, Johnson AJA, Holmes SP. DADA2: High-resolution sample inference from Illumina amplicon data. *Nat Methods*. 2016;13(7):581-583. doi:10.1038/nmeth.3869
57. Bolyen E, Rideout JR, Dillon MR, et al. Reproducible, interactive, scalable and extensible microbiome data science using QIIME 2. *Nat Biotechnol.Nature Publishing Group*. 2019;37(8):852-857. doi:10.1038/s41587-019-0209-9
58. Yilmaz P, Parfrey LW, Yarza P, et al. The SILVA and "all-species Living Tree Project (LTP)" taxonomic frameworks. *Nucleic Acids Res*. 2014;42(D1). doi:10.1093/nar/gkt1209
59. Morton JT, Marotz C, Washburne A, et al. Establishing microbial composition measurement standards with reference frames. *Nat Commun*. 2019;10(1). doi:10.1038/s41467-019-10656-5
60. McMurdie PJ, Holmes S. Phyloseq: An R Package for Reproducible Interactive Analysis and Graphics of Microbiome Census Data. *PLoS One*. 2013;8(4). doi:10.1371/journal.pone.0061217
61. Kenneth Helrich. *Official Methods for Analysis of the Association of Official Analytical Chemists*.; 1990.
62. Chaney AL, MEP. Modified Reagents for Determination of Urea and Ammonia. *Clin Chem*. 1962;8(2):130-132.

63. Holscher HD, Doligale JL, Bauer LL, et al. Gastrointestinal tolerance and utilization of agave inulin by healthy adults. *Food Funct*. 2014;5(6):1142-1149. doi:10.1039/c3fo60666j
64. Flickinger EA, Schreijen EMWC, Patil AR, et al. Nutrient digestibilities, microbial populations, and protein catabolites as affected by fructan supplementation of dog diets Get access Arrow. *J Anim Sci*. 2003;81(8):2008-2018.
65. Holscher HD, Chumpitazi BP, Dahl WJ, et al. Perspective: Assessing Tolerance to Nondigestible Carbohydrate Consumption. *Advances in Nutrition*. 2022;13(6):2084-2097. doi:10.1093/advances/nmac091
66. Maki K, Rains T, Kelley K, Cook C, Schild A, Gietl E. Fibermalt is well tolerated in healthy men and women at intakes up to 60 g/d: a randomized, double-blind, crossover trial. *Int J Food Sci Nutr*. 2013;63(3):274-281.
67. Tingley D, Yamamoto T, Hirose K, Keele L, Imai K. *Journal of Statistical Software Mediation: R Package for Causal Mediation Analysis*.; 2014. http://www.jstatsoft.org/
68. Chi WE, Huang S, Jeon M, Park ES, Melguizo T, Kezar A. A Practical Guide to Causal Mediation Analysis: Illustration With a Comprehensive College Transition Program and Nonprogram Peer and Faculty Interactions. *Front Educ (Lausanne)*. 2022;7. doi:10.3389/feduc.2022.886722
69. Sohn MB, Li H. Compositional mediation analysis for microbiome studies. *Annals of Applied Statistics*. 2019;13(1):661-681. doi:10.1214/18-AOAS1210
70. Aiken LS, West SG. Interaction Effects. In: *Encyclopedia of Statistics in Behavioral Science*. Wiley; 2005. doi:10.1002/0470013192.bsa306
71. Preacher KJ, Curran PJ, Bauer DJ. *Computational Tools for Probing Interactions in Multiple Linear Regression, Multilevel Modeling, and Latent Curve Analysis*. Vol 31.; 2006. http://www.quantpsy.org/.437
72. García-Bayona L, Comstock LE. Streamlined genetic manipulation of diverse bacteroides and parabacteroides isolates from the human gut microbiota. *mBio*. 2019;10(4). doi:10.1128/mBio.01762-19
73. Douglas GM, Maffei VJ, Zaneveld JR, et al. PICRUSt2 for prediction of metagenome functions. *Nat Biotechnol.Nature Research*. 2020;38(6):685-688. doi:10.1038/s41587-020-0548-6
74. Langille MGI, Zaneveld J, Caporaso JG, et al. Predictive functional profiling of microbial communities using 16S rRNA marker gene sequences. *Nat Biotechnol*. 2013;31(9):814-821. doi:10.1038/nbt.2676
75. Beghini F, McIver LJ, Blanco-Míguez A, et al. Integrating taxonomic, functional, and strain-level profiling of diverse microbial communities with biobakery 3. *Elife*. 2021;10. doi:10.7554/eLife.65088
76. Blanco-Míguez A, Beghini F, Cumbo F, et al. Extending and improving metagenomic taxonomic profiling with uncharacterized species using MetaPhlAn 4. *Nat Biotechnol*. 2023;41(11):1633-1644. doi:10.1038/s41587-023-01688-w
77. Segata N, Izard J, Waldron L, et al. Metagenomic biomarker discovery and explanation. *Genome Biol*. 2011;12(6). doi:10.1186/gb-2011-12-6-r60
78. Drula E, Garron ML, Dogan S, Lombard V, Henrissat B, Terrapon N. The carbohydrate-active enzyme database: Functions and literature. *Nucleic Acids Res*. 2022;50(D1):D571-D577. doi:10.1093/nar/gkab1045

79. Cantarel BI, Coutinho PM, Rancurel C, Bernard T, Lombard V, Henrissat B. The Carbohydrate-Active EnZymes database (CAZy): An expert resource for glycogenomics. *Nucleic Acids Res*. 2009;37(SUPPL. 1). doi:10.1093/nar/gkn663
80. Zheng J, Ge Q, Yan Y, Zhang X, Huang L, Yin Y. DbCAN3: Automated carbohydrate-Active enzyme and substrate annotation. *Nucleic Acids Res*. 2023;51(W1):W115-W121. doi:10.1093/nar/gkad328
81. Erdfelder E, FAul F, Buchner A, Lang AG. Statistical power analyses using G*Power 3.1: Tests for correlation and regression analyses. *Behav Res Methods*. 2009;41(4):1149-1160. doi:10.3758/BRM.41.4.1149
82. R Core Team. R: A language and environment for statistical computing. *Foundation for Statistical Computing*. Preprint posted online 2013.
83. H. Wickham. ggplot2: Elegant Graphics for Data Analysis. *Springer-VerlagNew York*. Published online 2016.
84. Kwak SK, Kim JH. Statistical data preparation: Management of missing values and outliers. *Korean J Anesthesiol.Korean Society of Anesthesiologists*. 2017;70(4):407-411. doi:10.4097/kjae.2017.70.4.407
85. Kafadar K. John Tukey and Robustness. *Statistical Science*. 2003;3(18(3)):319-331. doi:1076102419
86. Zhang X, Mallick H, Tang Z, et al. Negative binomial mixed models for analyzing microbiome count data. *BMC Bioinformatics*. 2017;18(1). doi:10.1186/s12859-016-1441-7
87. Sweeny AR, Lemon H, Ibrahim A, et al. A mixed-model approach for estimating drivers of microbiota community composition and differential taxonomic abundance. *mSystems*. Published online July 25, 2023. doi:10.1128/msystems.00040-23
88. Jamieson PE, Smart EB, Bouranis JA, et al. Gut enterotype-dependent modulation of gut microbiota and their metabolism in response to xanthohumol supplementation in healthy adults. *Gut Microbes*. 2024;16(1). doi:10.1080/19490976.2024.2315633
89. Zwietering MH, Jongenburger I, Rombouts FM, Van ' K, Riet T. *Modeling of the Bacterial Growth Curve PUm*.; 1990. https://journals.asm.org/journal/aem
90. Mallick H, Rahnavard A, McIver LJ, et al. Multivariable association discovery in population-scale meta-omics studies. *PLoS Comput Biol*. 2021;17(11). doi:10.1371/journal.pcbi.1009442
91. Yang C, Mai J, Cao X, Burberry A, Cominelli F, Zhang L. ggpicrust2: an R package for PICRUSt2 pre-dicted functional profile analysis and visualiza-tion. *Bioinformatics, YYYY*.:0-0. doi:10.1093/bioinformatics/xxxxx
92. Edwards CG, Walk AM, Thompson S V., et al. Effects of 12-week avocado consumption on cognitive function among adults with overweight and obesity. *International Journal of Psychophysiology*. 2020;148:13-24. doi:10.1016/j.ijpsycho.2019.12.006
93. Thompson S V., Bailey MA, Taylor AM, et al. Avocado Consumption Alters Gastrointestinal Bacteria Abundance and Microbial Metabolite Concentrations among Adults with Overweight or Obesity: A Randomized Controlled Trial. *Journal of Nutrition*. 2021;151(4):753-762. doi:10.1093/jn/nxaa219
94. Mehren A, Luque CD, Brandes M, et al. Intensity-dependent effects of acute exercise on executive function. *Neural Plast*. 2019;2019. doi:10.1155/2019/8608317

95. Timm DA, Thomas W, Boileau TW, Williamson-Hughes PS, Slavin JL. Polydextrose and soluble corn fiber increase five-day fecal wet weight in healthy men and women. *Journal of Nutrition*. 2013;143(4):473-478. doi:10.3945/jn.112.170118
96. Hooda S, Vester Boler BM, Rossoni Serao MC, et al. 454 pyrosequencing reveals a shift in fecal microbiota of healthy adult men consuming polydextrose or soluble corn fiber. *Journal of Nutrition*. 2012;142(7):1259-1265. doi:10.3945/jn.112.158766
97. Shimizu H, Nakajima M, Miyanaga A, et al. Characterization and Structural Analysis of a Novel exo-Type Enzyme Acting on β-1,2-Glucooligosaccharides from Parabacteroides distasonis. *Biochemistry*. 2018;57(26):3849-3860. doi:10.1021/acs.biochem.8b00385
98. Ducarmon QR, Karcher N, Tytgat HLP, et al. Large-scale computational analyses of gut microbial CAZyme repertoires enabled by Cayman. Preprint posted online January 8, 2024. doi:10.1101/2024.01.08.574624
99. Lapébie P, Lombard V, Drula E, Terrapon N, Henrissat B. Bacteroidetes use thousands of enzyme combinations to break down glycans. *Nat Commun*. 2019;10(1). doi:10.1038/s41467-019-10068-5
100. Gibson GR, Hutkins R, Sanders ME, et al. Expert consensus document: The International Scientific Association for Probiotics and Prebiotics (ISAPP) consensus statement on the definition and scope of prebiotics. *Nat Rev Gastroenterol Hepatol.Nature Publishing Group*. 2017;14(8):491-502. doi:10.1038/nrgastro.2017.75
101. Goel A, Shete O, Goswami S, et al. Toward a health-associated core keystone index for the human gut microbiome. *Cell Rep*. 2025;44(3):115378. doi:10.1016/j.celrep.2025.115378
102. Cui Y, Zhang L, Wang X, et al. Roles of intestinal Parabacteroides in human health and diseases. *FEMS Microbiol Lett.Oxford University Press*. 2022;369(1). doi:10.1093/femsle/fnac072
103. Cuffaro B, Boutillier D, Desramaut J, et al. Characterization of Two Parabacteroides distasonis Candidate Strains as New Live Biotherapeutics against Obesity. *Cells*. 2023;12(9). doi:10.3390/cells12091260
104. Ezeji JC, Sarikonda DK, Hopperton A, et al. Parabacteroides distasonis: intriguing aerotolerant gut anaerobe with emerging antimicrobial resistance and pathogenic and probiotic roles in human health. *Gut Microbes.Bellwether Publishing, Ltd.* 2021;13(1). doi:10.1080/19490976.2021.1922241
105. Liang Z, Di N, Li L, Yang D. Gut microbiota alterations reveal potential gut–brain axis changes in polycystic ovary syndrome. *J Endocrinol Invest*. 2021;44(8):1727-1737. doi:10.1007/s40618-020-01481-5
106. Wei W, Wong CC, Jia Z, et al. Parabacteroides distasonis uses dietary inulin to suppress NASH via its metabolite pentadecanoic acid. *Nat Microbiol*. 2023;8(8):1534-1548. doi:10.1038/s41564-023-01418-7
107. Liu D, Zhang S, Li S, et al. Indoleacrylic acid produced by Parabacteroides distasonis alleviates type 2 diabetes via activation of AhR to repair intestinal barrier. *BMC Biol*. 2023;21(1). doi:10.1186/s12915-023-01578-2
108. Keaney J, Campbell M. The dynamic blood-brain barrier. *FEBS Journal*. 2015;282(21):4067-4079. doi:10.1111/febs.13412
109. Van Dokkum W, Wezendonk B, Srikumar TS, Van Den Heuvel EGHM. Effect of nondigestible oligosaccharides on large-bowel functions, blood lipid concentrations and

glucose absorption in young healthy male subjects. *Eur J Clin Nutr*. 1999;53(1):1-7. doi:10.1038/sj.ejcn.1600668

110. Pedersen A, Sandström B, Van Amelsvoort JMM. The effect of ingestion of inulin on blood lipids and gastrointestinal symptoms in healthy females. *British Journal of Nutrition*. 1997;78(2):215-222. doi:10.1079/bjn19970141

111. Dalile B, La Torre D, Kalc P, et al. Extruded Wheat Bran Consumption Increases Serum Short-Chain Fatty Acids but Does Not Modulate Psychobiological Functions in Healthy Men: A Randomized, Placebo-Controlled Trial. *Front Nutr*. 2022;9. doi:10.3389/fnut.2022.896154

112. Wang S, Mu L, Yu C, et al. Microbial collaborations and conflicts: unraveling interactions in the gut ecosystem. *Gut Microbes*.*Taylor and Francis Ltd.* 2024;16(1). doi:10.1080/19490976.2023.2296603

113. Takada T, Kurakawa T, Tsuji H, Nomoto K. Fusicatenibacter saccharivorans gen. nov., sp. nov., isolated from human faeces. *Int J Syst Evol Microbiol*. 2013;63(PART10):3691-3696. doi:10.1099/ijs.0.045823-0

114. Li J, Zhu S, Wang Y, et al. Metagenomic association analysis of cognitive impairment in community-dwelling older adults. *Neurobiol Dis*. 2023;180. doi:10.1016/j.nbd.2023.106081

115. Loh JS, Mak WQ, Tan LKS, et al. Microbiota–gut–brain axis and its therapeutic applications in neurodegenerative diseases. *Signal Transduct Target Ther*.*Springer Nature*. 2024;9(1). doi:10.1038/s41392-024-01743-1

1078 **Tables**

1079 **Table 1.** Baseline demographic and clinical characteristics of participants randomized to
1080 treatment counterbalanced.
1081

	Overall N = 42	**Maltodextrin** N = 21	**Soluble Corn Fiber** N = 21
Education			
High School Graduate	2 (4.8%)	0 (0%)	2 (9.5%)
Some college	6 (14%)	3 (14%)	3 (14%)
Bachelor's Degree	13 (31%)	8 (38%)	5 (24%)
Advanced Degree	21 (50%)	10 (48%)	11 (52%)
Ethnicity			
Asian	6 (14%)	3 (14%)	3 (14%)
Black or African American	3 (7.1%)	1 (4.8%)	2 (9.5%)
Mixed or Other	1 (2.4%)	0 (0%)	1 (4.8%)
White (Caucasian)	32 (76%)	17 (81%)	15 (71%)
Latino	1 (2.4%)	1 (4.8%)	0 (0%)
Sex			
Female	28 (67%)	15 (71%)	13 (62%)
Male	14 (33%)	6 (29%)	8 (38%)
Age (years)	56.2 ± 7.3	54.8 ± 6.2	57.5 ± 8.2
Fiber per 1000kcal	11.4 ± 3.4	12.0 ± 3.3	10.8 ± 3.5
BMI (kg/m²)	25.9 ± 4.0	25.4 ± 3.7	26.3 ± 4.2
Income			
Less than $10,000	1 (2.4%)	0 (0%)	1 (4.8%)
$11,000-20,000	0 (0%)	0 (0%)	0 (0%)
$21,000-30,000	0 (0%)	0 (0%)	0 (0%)
$31,000-40,000	3 (7.1%)	1 (4.8%)	2 (9.5%)
$41,000-50,000	3 (7.1%)	1 (4.8%)	2 (9.5%)
$51,000-60,000	3 (7.1%)	2 (9.5%)	1 (4.8%)
$61,000-70,000	4 (9.5%)	1 (4.8%)	3 (14%)
$71,000-80,000	5 (12%)	4 (19%)	1 (4.8%)
$81,000-90,000	1 (2.4%)	1 (4.8%)	0 (0%)
$91,000-100,000	7 (16.7%)	4 (19%)	3 (14%)
Greater than $100,000	15 (35.7%)	7 (33%)	8 (38%)

1082
1083 Baseline characteristics of participants enrolled and randomized into the clinical trial (N = 42), stratified by initial
1084 treatment assignment. Continuous variables are reported as mean ± standard deviation; categorical variables are
1085 reported as number of participants and percentage within each group [n (%)].
1086

1087

Table 2. Behavioral and ERP measures during the flanker task across treatment and time.

	Maltodextrin		Soluble Corn Fiber					
	PRE	**POST**	**PRE**	**POST**	**Treatment x Time (Model Estimates)**			
Behavioral Flanker	Mean ± SEM *(n)*	Mean ± SEM *(n)*	Mean ± SEM *(n)*	Mean ± SEM *(n)*	β	SE	95% CI	*p*
Accuracy (%)								
Congruent	96.9 ± 0.52 *(39)*	95.5 ± 1.37 *(39)*	97.0 ± 0.48 *(40)*	97.6 ± 0.45 *(40)*	0.65	0.81	[-0.93, 2.23]	0.42
Incongruent	92.4 ± 1.00 *(39)*	92.0 ± 1.53 *(39)*	93.6 ± 0.79 *(40)*	94.4 ± 0.70 *(40)*	-0.68	1.10	[-2.82, 1.46]	0.53
Reaction Time (ms)								
Congruent	395. ± 5.79 *(39)*	**398. ± 6.69**[a] *(39)*	400.71 ± 6.22 *(40)*	**389. ± 5.52**[b] *(40)*	-13.8	5.51	[-24.5, -3.03]	**0.01***
Incongruent	431. ± 6.62 *(39)*	**437. ± 7.77**[a] *(39)*	435.43 ± 6.88 *(40)*	**424. ± 6.35**[b] *(40)*	-16.4	6.57	[-29.2, -3.62]	**0.01***
ERP Flanker								
Amplitude (μV)								
Congruent	5.96 ± 1.73 *(39)*	6.78 ± 0.68 *(36)*	6.64 ± 0.60 *(39)*	7.07 ± 0.77 *(37)*	0.88	1.18	[-2.22, 1.01]	0.46
Incongruent	6.36 ± 1.64 *(39)*	6.77 ± 0.69 *(36)*	7.14 ± 0.65 *(39)*	7.50 ± 0.79 *(37)*	1.08	1.10	[-1.06, 3.24]	0.33
Peak Latency (ms)								
Congruent	386. ± 6.71 *(39)*	399. ± 10.18 *(36)*	394. ± 7.29 *(39)*	398. ± 7.99 *(37)*	-6.16	0.32	[-31.1, 18.7]	0.67
Incongruent	424. ± 8.34 *(39)*	443. ± 11.70 *(36)*	438. ± 9.90 *(39)*	429. ± 8.27 *(37)*	-23.0	15.4	[-53.2, 6.81]	0.14

Values are means ± standard error of the mean (SEM) and sample size (n) across congruencies at each timepoint. Measures include accuracy (%), reaction time (ms), P3 amplitude (μV), and P3 peak latency (ms). Linear mixed-effect models included participant ID as a random effect, and the fixed effects of treatment, time, and their interaction. Reported are the treatment-by-time interaction estimates (β, Standard Error (SE), 95% confidence interval (CI), *p*-values). *Post-hoc* pairwise comparisons were conducted within each congruency when a treatment-by-time interaction met the significance threshold ($p < 0.05$), with *p*-values adjusted using the Benjamin-Hochberg procedure. Superscripts (a, b) denote significant *post-hoc* differences within congruency trials between treatments and time. Significance threshold *p*: '***' <0.001, '**' <0.01, '*' <0.05, '†' <0.1.

1097 **Table 3.** 16S Alpha diversity and differential abundance of genera across treatment and time.

	Maltodextrin		**Soluble Corn Fiber**					
	PRE	**POST**	**PRE**	**POST**	**Treatment x Time (Model Summary)**			
16S ASVs	Mean ± SEM *(n)*	Mean ± SEM *(n)*	Mean ± SEM *(n)*	Mean ± SEM *(n)*	β	SE	95% CI	FDR *p*
Genera (% of sequence)								
Bacteroides	25.2 ± 1.77 *(38)*	23.7 ± 1.90 *(38)*	27.3 ± 2.06 *(37)*	22.6 ± 2.07 *(37)*	-0.15	0.10	[-0.34, 0.05]	0.11
Faecalibacterium	10.2 ± 1.02 *(38)*	10.1 ± 1.11 *(38)*	8.66 ± 1.15 *(37)*	11.0 ± 1.30 *(37)*	0.23	0.21	[-0.18, 0.64]	0.47
Parabacteroides	2.52 ± 0.35[a] *(38)*	**2.06 ± 0.24[a]** *(38)*	2.09 ± 0.26[a] *(37)*	**8.37 ± 0.98[b]** *(37)*	**1.44**	**0.22**	[1.01, 1.88]	**<0.001*** **
Alistipes	3.46 ± 0.51 *(38)*	2.82 ± 0.35 *(38)*	3.88 ± 0.59 *(37)*	3.96 ± 0.69 *(37)*	0.08	0.20	[-0.31, 0.46]	0.50
Blautia	3.76 ± 0.50 *(38)*	4.52 ± 0.61 *(38)*	3.54 ± 0.42 *(37)*	3.24 ± 0.50 *(37)*	-0.27	0.13	[-0.52, -0.02]	0.10†
Agathobacter	4.16 ± 0.88 *(38)*	5.97 ± 1.17 *(38)*	3.99 ± 0.85 *(37)*	2.80 ± 0.58 *(37)*	-0.46	0.23	[-0.91, 0.01]	0.11
Subdoligranulum	2.31 ± 0.29 *(38)*	2.54 ± 0.38 *(38)*	3.24 ± 0.58 *(37)*	2.69 ± 0.49 *(37)*	-0.24	0.22	[-0.68, 0.19]	0.83
Prevotella	0.87 ± 0.41 *(38)*	1.64 ± 0.74 *(38)*	1.60 ± 0.89 *(37)*	2.13 ± 1.04 *(37)*	-0.22	0.30	[-0.81, 0.37]	0.53
Dialister	1.34 ± 0.44[a] *(38)*	**1.46 ± 0.51[a]** *(38)*	0.93 ± 0.34[a] *(37)*	**2.10 ± 0.63[b]** *(37)*	1.06	0.39	[0.29, 1.83]	**0.02***
Bifidobacterium	2.50 ± 0.53 *(38)*	2.69 ± 0.53 *(38)*	2.12 ± 0.52 *(37)*	2.09 ± 0.41 *(37)*	0.09	0.31	[-0.51, 0.70]	0.92
Fusicatenibacter	0.60 ± 0.10[a] *(38)*	**0.67 ± 0.09[a]** *(38)*	0.53 ± 0.11[a] *(37)*	**1.79 ± 0.28[b]** *(37)*	1.10	1.10	[0.59, 1.61]	**<0.001*** **
Alpha Diversity Metrics								
Richness	439.9 ± 19.8[a] *(38)*	**438.7 ± 18.2[a]** *(38)*	443.6 ± 17.6[a] *(37)*	**413.7 ± 18.6[b]** *(37)*	-0.76	0.29	[-1.32, -0.19]	**0.03***
Shannon	3.89 ± 0.06 *(38)*	3.88 ± 0.06 *(38)*	3.81 ± 0.06 *(37)*	3.71 ± 0.07 *(37)*	-0.08	0.07	[-0.22, 0.06]	0.26
Faith's PD	104.7 ± 1.62 *(38)*	103.9 ± 1.54 *(38)*	105.23 ± 1.54 *(37)*	101.9 ± 1.80 *(37)*	-2.43	1.28	[-4.93, 0.06]	0.09†

1098
1099 Values are means ± standard error of the mean (SEM) and sample size (*n*) across each timepoint. For differential abundance of 16S genera, a generalized linear
1100 mixed-effect negative binomial model included participant ID as a random effect, and the fixed effects of treatment, time, and their interaction. Reported are the
1101 treatment-by-time interaction log-scaled estimates (β, Standard Error (SE), 95% confidence interval (CI), FDR-adjusted *p*-values). For alpha diversity metrics,
1102 linear mixed-effect model. Reported are the treatment-by-time interaction estimates. *Post-hoc* was conducted if a interaction met the significance threshold ($p <$
1103 0.05), *p*-values adjusted using the Benjamin-Hochberg procedure. Superscripts (a, b) denote significant *post-hoc* differences between treatments and time.
1104 Significance threshold *p*: '***' <0.001, '**' <0.01, '*' <0.05, '†' <0.1.
1105

1106 **Table 4.** Fecal volatile fatty acids across treatment and time.

	Maltodextrin		Soluble Corn Fiber		Treatment x Time (Model Estimates)			
	PRE	**POST**	**PRE**	**POST**				
Fermentation end-products (µmol/g DMB)	Mean ± SEM *(n)*	Mean ± SEM *(n)*	Mean ± SEM *(n)*	Mean ± SEM *(n)*	β	SE	95% CI	*p*
SCFAs								
Butyrate	43.3 ± 4.56 *(38)*	43.9 ± 5.26 *(37)*	38.8 ± 4.58 *(37)*	40.1 ± 3.18 *(37)*	0.10	0.13	[-0.16, 0.37]	0.44
Acetate	176. ± 13.9 *(38)*	182. ± 13.5 *(37)*	165. ± 13.2 *(37)*	202. ± 14.9 *(37)*	0.16	0.11	[-0.04, 0.36]	0.14
Propionate	48.1 ± 3.98 *(38)*	50.8 ± 4.40 *(37)*	47.5 ± 4.32 *(37)*	55.6 ± 4.72 *(37)*	0.14	0.10	[-0.09, 0.36]	0.23
Total SCFAs	267. ± 21.5 *(38)*	273. ± 21.97 *(37)*	255. ± 20.6 *(37)*	298. ± 22.3 *(37)*	0.15	0.11	[-0.05, 0.36]	0.15
BCFAs								
Valerate	6.44 ± 0.59 *(38)*	5.99 ± 0.47 *(37)*	6.00 ± 0.47 *(37)*	5.68 ± 0.48 *(37)*	-0.06	0.16	[-0.36, 0.24]	0.71
Isobutyrate	6.62 ± 0.54 *(38)*	5.97 ± 0.39 *(36)*	6.29 ± 0.52 *(37)*	5.22 ± 0.33 *(37)*	-0.08	0.11	[-0.30, 0.14]	0.48
Isovalerate	9.49 ± 0.82 *(38)*	8.30 ± 0.57 *(36)*	8.66 ± 0.69 *(37)*	7.35 ± 0.54 *(37)*	-0.04	0.14	[-0.31, 0.22]	0.75
Total BCFAs	22.6 ± 1.83 *(38)*	20.4 ± 1.31 *(37)*	21.0 ± 1.56 *(37)*	18.3 ± 1.14 *(37)*	-0.03	0.20	[-0.43, 0.36]	0.87

1107
1108 Values are descriptive means ± standard error of the mean (SEM) and sample size (n) across each timepoint. Total SCFAs and BCFAs are pooled measures, within
1109 respective category. Linear mixed-effect models included participant ID as a random effect, and the fixed effects of treatment, time, and their interaction. Reported
1110 are the treatment-by-time interaction estimates (β, Standard Error (SE), 95% confidence interval (CI), *p*-values).

1111 **Table 5.** Self-reported gastrointestinal symptoms across treatment and time.

	Maltodextrin		**Soluble Corn Fiber**		
	PRE	**POST**	**PRE**	**POST**	
GI Symptoms	Median [IQR] *(n)*	Median [IQR] *(n)*	Median [IQR] *(n)*	Median [IQR] *(n)*	*p*
Gas	1.57 [0.84] *(39)*	**1.43 [1.00]** *(39)*	1.57 [0.97] *(38)*	**1.93 [1.00]** *(38)*	**0.01***
Cramping	1.00 [0.00] *(39)*	1.00 [0.00] *(39)*	1.00 [0.00] *(38)*	1.00 [0.14] *(38)*	0.91
Bloating	1.00 [0.14] *(39)*	1.00 [0.14] *(39)*	1.00 [0.14] *(38)*	1.00 [0.32] *(38)*	0.05†
Nausea	1.00 [0.00] *(39)*	1.00 [0.00] *(39)*	1.00 [0.00] *(38)*	1.00 [0.00] *(38)*	0.17
Reflux	1.00 [0.00] *(39)*	1.00 [0.00] *(39)*	1.00 [0.03] *(38)*	1.00 [0.00] *(38)*	0.84
Rumbling	1.00 [0.16] *(39)*	1.00 [0.16] *(39)*	1.00 [0.17] *(38)*	1.00 [0.41] *(38)*	0.68
Burping	1.00 [0.16] *(39)*	1.00 [0.00] *(39)*	1.00 [0.28] *(38)*	1.00 [0.17] *(38)*	0.70

1112
1113 Values are descriptive median ± interquartile range (IQR) and sample size (n) across each timepoint. Symptom
1114 severity was rated on a 4-point scale (1 = Absent, 2 = Mild, 3 = Moderate, 4 = Severe). Reported values include *p*-
1115 values from the paired Wilcoxon Signed-Rank tests. Significance threshold *p*: '*' <0.05, '†' <0.1.
1116

1117

1118

1119

1120

1121

1122

1123

1124

1125

1126

1127 **Table 6.** Mediation of SCF-related changes in Flanker reaction times through fecal SCFAs and
1128 16S taxa.

			Nonparametric Bootstrap Confidence Intervals with Percentile		
Mediator	**Flanker Task**	**Effect**	**β**	**[95% CI]**	***p***
Acetate	Congruent RT	ACME	-0.57	[-2.51, 0.87]	0.48
		ADE	-13.42	[-23.7, -3.23]	0.01*
		Total effect	-13.99	[-14.0, -24.4]	0.009**
		Proportion Mediated	4.09%	[-0.08, 0.21]	0.48
	Incongruent RT	ACME	-0.44	[-2.87, 1.61]	0.72
		ADE	-17.03	[-29.4, -4.38]	0.008**
		Total effect	-17.47	[-30.1, -4.63]	0.007**
		Proportion Mediated	2.51%	[-0.11, 0.19]	0.72
Propionate	Congruent RT	ACME	-0.64	[-2.39, 0.81]	0.43
		ADE	-13.39	[-23.9, -3.30]	0.01*
		Total effect	-14.03	[-24.4, -3.78]	0.008**
		Proportion Mediated	4.57%	[-0.28, 0.08]	0.43
	Incongruent RT	ACME	-0.38	[-4.32, 0.78]	0.22
		ADE	-17.11	[-23.0, -2.36]	0.03*
		Total effect	-17.49	[-24.3, -3.77]	0.01*
		Proportion Mediated	2.22%	[-0.11, 0.54]	0.23
Parabacteroides	Congruent RT	ACME	-0.15	[-9.31, 4.27]	0.93
		ADE	-13.85	[-25.9, 0.39]	0.06
		Total effect	-14.00	[-24.3, -3.83]	0.008**
		Proportion Mediated	1.06%	[-0.36, 1.02]	0.93
	Incongruent RT	ACME	-0.48	[-12.64, 4.53]	0.86
		ADE	-17.00	[-30.5, 0.20]	0.03*
		Total effect	-17.48	[-30.0, -4.80]	0.01*
		Proportion Mediated	2.75%	[-0.34, 0.96]	0.86
Fusicatenibacter	Congruent RT	ACME	-1.40	[-4.98, 0.65]	0.19
		ADE	-12.63	[-23.0, -2.28]	0.02*
		Total effect	-14.03	[-24.3, -3.84]	0.007**
		Proportion Mediated	10.0%	[-0.06, 0.50]	0.19
	Incongruent RT	ACME	-0.72	[-4.98, 2.16]	0.59
		ADE	-16.75	[-29.1, -3.85]	0.01*
		Total effect	-17.47	[-30.0, -4.79]	0.007**
		Proportion Mediated	4.1%	[-0.18, 0.35]	0.59
Dialister	Congruent RT	ACME	0.44	[-0.89, 3.47]	0.52
		ADE	-14.44	[-25.4, -4.22]	0.006**
		Total effect	-14.00	[-24.2, -3.75]	0.007**
		Proportion Mediated	-3.15%	[-0.33, 0.08]	0.53
	Incongruent RT	ACME	0.67	[-1.26, 4.95]	0.52
		ADE	-18.15	[-31.8, -5.12]	0.007**
		Total effect	-17.49	[-30.0, -4.70]	0.007**
		Proportion Mediated	-3.8%	[-0.35, 0.11]	0.53

1129 Mediation analysis was conducted using nonparametric bootstrapped linear regression models (R; *mediation*) to
1130 estimate the average causal mediation effect (ACME), average direct effect (ADE), and total effects of treatment on
1131 changes in reaction times (RT) Reported are the model estimates (β), Standard Error (SE), 95% confidence interval
1132 (CI), (n = 37). Proportion mediated indicates the percentage of the total effect explained by the ACME pathway.
1133 Significance threshold p: '***' <0.001, '**' <0.01, '*' <0.05, '†' <0.1.

Table 7. Moderation influence of fecal SCFAs and 16S genera on SCF-related changes in Flanker reaction times.

Moderator	Flanker Task	Treatment x Moderator (Model Summary)						
		ΔR^2	Adj. ΔR^2	β	SE	t	[95% CI]	*p*
Acetate	Congruent RT	0.11	0.07	3.13	5.62	0.56	[-8.08, 14.3]	0.58
	Incongruent RT	0.10	0.06	2.21	6.80	0.33	[-11.4, 15.8]	0.75
Propionate	Congruent RT	0.11	0.07	0.43	5.60	0.08	[-10.76, 11.6]	0.94
	Incongruent RT	0.10	0.06	0.40	6.80	0.06	[-13.17, 14.0]	0.95
Parabacteroides	Congruent RT	**0.16**	0.12	**-19.8**	10.12	-1.95	[-40.0, 0.43]	**0.05***
	Incongruent RT	**0.15**	0.12	**-25.1**	12.24	-2.05	[-49.5, 0.63]	**0.04***
Fusicatenibacter	Congruent RT	0.10	0.06	-1.31	13.48	-0.10	[-28.2, 25.6]	0.92
	Incongruent RT	0.11	0.07	11.49	16.20	0.71	[-20.9, 43.8]	0.49
Dialister	Congruent RT	0.11	0.07	-4.49	7.39	-0.61	[-19.2, 10.3]	0.55
	Incongruent RT	0.10	0.06	0.23	8.98	0.03	[-17.7, 18.2]	0.98

Moderation analysis was conducted using linear regression models testing if changes in moderators explain variability in flanker reaction times (RT). Each model includes treatment, Δ moderator, and its interaction. Reported are the treatment-by-moderator estimates (β, Standard Error (SE), 95% confidence interval (CI), *p*-values). The ΔR^2 and adjusted ΔR^2 columns show the variance explained by the full model. Statistical threshold for *p*: '***' <0.001, '**' <0.01, '*' <0.05, '†' <0.1.

1148 **Table 8.** Summary of Responder analysis across the SCF intervention.

	Non-Responder		Responder	
	PRE	**POST**	**PRE**	**POST**
Pilot Analyses	Mean ± SD *(n)*	Mean ± SD *(n)*	Mean ± SD *(n)*	Mean ± SD *(n)*
Genera (% of Sequences)				
Parabacteroides	0.43 ± 0.64 *(3)*	*ND (3)*	1.04 ± 0.33 *(3)*	14.61 ± 2.82 *(3)*
Dialister	1.50 ± 0.79 *(3)*	3.18 ± 3.25 *(3)*	0.25 ± 0.43 *(3)*	*ND (3)*
Fusicatenibacter	0.48 ± 0.45 *(3)*	2.69 ± 2.77 *(3)*	1.24 ± 1.65 *(3)*	1.35 ± 1.34 *(3)*
Species (% of Sequences)				
P. distasonis	0.01 ± 0.01 *(3)*	*ND (3)*	0.49 ± 0.17 *(3)*	11.38 ± 1.47 *(3)*
P. merdae	0.41 ± 0.63 *(3)*	*ND (3)*	0.55 ± 0.50 *(3)*	3.23 ± 3.67 *(3)*
P. faecis	0.01 ± 0.01 *(3)*	*ND (3)*	*ND (3)*	*ND (3)*
D. invisus	0.73 ± 0.73 *(3)*	1.00 ± 1.74 *(3)*	0.25 ± 0.43 *(3)*	*ND (3)*
D. hominis	0.77 ± 1.34 *(3)*	2.17 ± 3.75 *(3)*	*ND (3)*	*ND (3)*
F. saccharivorans	0.48 ± 0.45 *(3)*	2.69 ± 2.77 *(3)*	1.24 ± 1.65 *(3)*	1.35 ± 1.34 *(3)*
Flanker Reaction Time (ms)				
Congruent	428.9 ± 24.4 *(3)*	396.7 ± 11.6 *(3)*	363.0 ± 50.2 *(3)*	362.1 ± 42.7 *(3)*
Incongruent	456.6 ± 3.9 *(3)*	424.9 ± 14.4 *(3)*	403.9 ± 60.2 *(3)*	401.1 ± 50.2 *(3)*
SCFAs (µmol/g DMB)				
Acetate	153.8 ± 60.9 *(3)*	225.4 ± 88.9 *(3)*	180.2 ± 95.1 *(3)*	246.6 ± 59.1 *(3)*
Propionate	28.47 ± 12.2 *(3)*	57.02 ± 23.7 *(3)*	51.89 ± 23.6 *(3)*	72.81 ± 27.2 *(3)*
Demographics				
Age *(year)*	53.7 ± 7.2 *(3)*		54.3 ± 2.5 *(3)*	

1149
1150 Descriptive analyses of microbial responders and non-responders during the SCF intervention subsampled from the
1151 study. Data are presented as mean ± standard deviation (SD) and sample size (*n*). Metaphlan4 was used for genus and
1152 species relative abundance values (%). Species initials correspond as follows: *P* = *Parabacteroides*, *D* = *Dialister*,
1153 and *F* = *Fusicatenibacter*.
1154

1155

1156

1157

1158 **Figure Legend**

1159 **Figure 1. Study design timeline and sample collection procedures.** Participants completed six
1160 laboratory visits across two 4-week intervention periods separate by a washout. Visit 1: Eligibility
1161 (screening, consent/surveys); if eligible, they were randomized and scheduled (~2 weeks) for their
1162 Visit 2 with stool collection and diet record deployed for Visit 3 first intervention baseline. Visit
1163 2: Practice/familiarization sessions with EEG cap placement, scheduled ~1 week before to testing
1164 visit. Visits 3 and 5: Pre-intervention testing days with the full EEG-based cognitive battery. Visits
1165 4 and 6: Post-intervention follow-ups with the same testing battery. Stools samples were collected
1166 over the final 5-days of each intervention period and returned at the subsequent testing visit.
1167 (*Figure created using BioRender)*
1168
1169 **Figure 2. CONSORT flow diagram of recruitment, randomization, and retention.** Each "*n*"
1170 indicates the number of participants at each stage of the study. Participants were randomized to
1171 maltodextrin (CON) or soluble corn fiber (SCF) in a counterbalanced crossover design. (*Figure*
1172 *created using BioRender)*
1173
1174 **Figure 3. Flanker task reaction times for both congruencies across each timepoint.** Raw
1175 distributions (left) and model-derived estimated marginal means (right) of reaction times (RT,
1176 ms) are shown for (**A**) congruent trials (top row) and (**B**) incongruent trials (bottom row) across
1177 treatment and time. Statistical significance derived from *post-hoc* pairwise comparisons. FDR-
1178 adjusted *p*-values annotated as follows: ** < 0.01; * < 0.05; † < 0.1.
1179
1180 **Figure 4. 16S microbiota composition across condition and participants.** (**A**) First row shows
1181 relative abundance (%) of the top 5 for phyla (left) and top 10 for genera (right) across the
1182 interventions averaged within conditions. Color gradient for genera correspond to their parent
1183 phylum. (**B**) 16S differential abundance volcan plot shows glmm model interaction estimates with
1184 effect size increasing from the center dashed vertical line). The y-axis corresponds to the
1185 significance of the genera, higher meaning more significant, with a horizontal dashed line
1186 indicating the FDR $p = 0.05$ threshold. The waterfall plot (**C**) highlights patterns from statistically
1187 relevant genera at the individual level.
1188
1189 **Figure 5. Distribution and *post-hoc* comparison of 16S selected genera.** Relative abundances
1190 (% of sequences) on the left and estimated marginal pairwise comparisons (Emmeans, right; log
1191 scale) of *Parabacteroides* (A), *Fusicatenibacter* (B), and *Dialister* (C) across conditions. *Post-hoc*
1192 analyses show FDR-adjusted *p* between treatment at endpoint. Statistical significance is annotated
1193 as follows: *** < 0.001; ** < 0.01; * < 0.05; † < 0.1.
1194
1195 **Figure 6. Spearman correlation heatmap of reaction times, fecal SCFAs, and 16S genera**
1196 **following soluble corn fiber intervention.** Heatmap displays Spearman's coefficients (ρ)
1197 between the markers of interest and the flanker task reaction times ($n = 37$; SCF arm only). Positive
1198 correlations are orange, negative correlations blue, with intensity reflecting the magnitude.
1199 Spearman *p*-values were FDR adjusted. Statistical significances are annotated as follows: *p* ***
1200 < 0.001, † < 0.1.
1201

1202 **Figure 7. Interaction between 16S *Parabacteroides* and SCF effect on RTs.** Moderation
1203 outcomes, with the top row (**A**) for congruent RTs, and the bottom row (**B**) for incongruent RTs
1204 (ΔRT, ms) plotted as a function of change in the relative abundance of *Parabacteroides* (z-scored).
1205 On the left, lines represent model-predicted simple slopes for maltodextrin (blue) and SCF
1206 (orange) groups with vertical dotted lines marking the conditional effects at low (-1 standard
1207 deviation (SD)), centered mean, and high (+1 SD) of Δ*Parabacteroides*. On the right, panels show
1208 estimated pairwise differences (SCF-CON) from emmeans contrasts of the moderator values; the
1209 vertical line indicates no change, crossing indicates no statistical significance. Significance
1210 threshold p * <0.05.
1211
1212 **Figure 8. Growth rates of *Parabacteroides distasonis* cultured in M9 supplement with SCF**
1213 **compared to controls.** The relative log growth curve of *P. distasonis* (A) in M9 minimal medium
1214 supplemented with different carbohydrate sources. OD_0 represents the initial optical density
1215 (OD_{600}) at time zero. Each curve represents a mean biological replicate (N = 3), and error bars
1216 indicate propagated standard deviations. The mean growth rate (B), calculated as the slope of
1217 ln(OD) over sequential 2-hour intervals, cut off at 10-hrs. Bars represent average growth rate
1218 across replicates. Significance threshold p: '***' < 0.001, '**' < 0.01, '*' < 0.05, '†' < 0.1, 'NS'
1219 > 0.1.
1220
1221 **Figure 9. Abundance of carbohydrate metabolism-associated gene families comparison**
1222 **between responders and non-responders at endpoint of the SCF intervention.** Heatmap
1223 displaying the abundance of carbohydrate metabolism-related gene families annotated by
1224 HUMAnNv3.0 across six participants (N = 6), stratified by responder (R1–R3) and non-responder
1225 (NR1–NR3) status. Genes families shown (rows) were selected from a total of 1,180 unique
1226 carbohydrate-associated gene families based on a $\log_2$ fold change > 2 in mean abundance between
1227 responders and non-responders [log2(R/NR)]. The top 40 gene families are presented. Abundance
1228 values were row-scaled using Z-score normalization to emphasize relative variation across
1229 samples. Orange indicates higher abundance, and blue indicates lower abundance for each gene.
1230
1231 **Figure 10. Responders' species-level profile contributions over time to carbohydrate**
1232 **metabolism gene family abundances.** Heatmaps showing the contribution of individual species
1233 (columns) to the abundance of 40 carbohydrate metabolism-associated gene families (rows) of
1234 microbial responders. The top panel (A) shows the baseline timepoint while the bottom panel (B)
1235 shows the endpoint of the SCF intervention. Gene abundance was row-normalized using Z-scores
1236 to highlight species-level contributions, with orange indicating higher and blue indicating lower
1237 abundance for each gene.
1238

1239

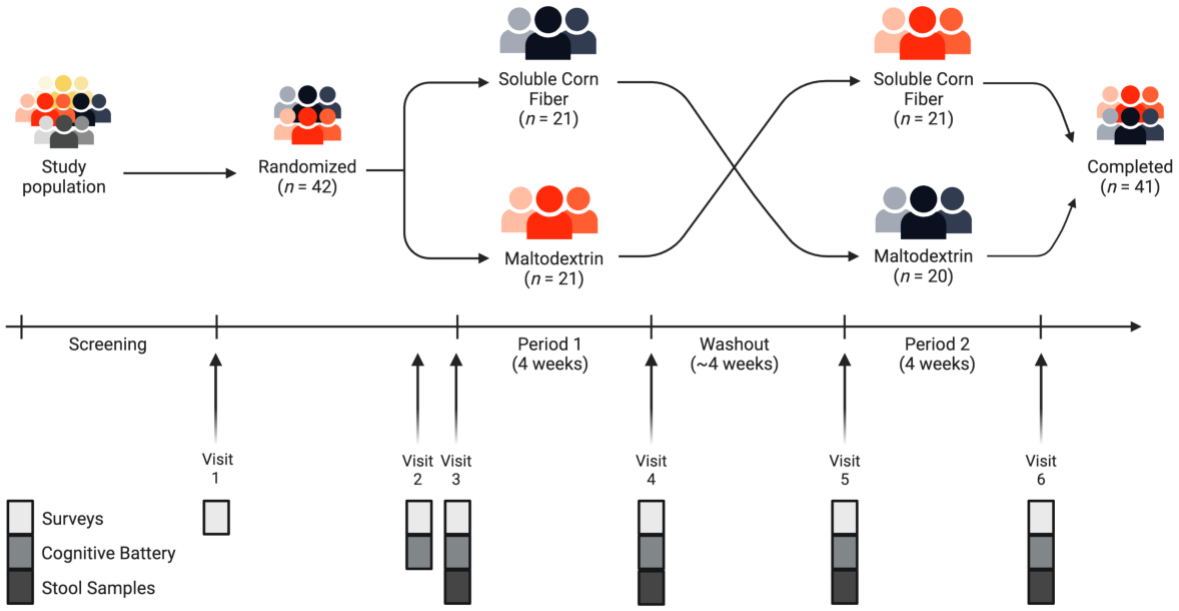

Figure 1. Study design timeline and sample collection procedures. Participants completed six laboratory visits across two 4-week intervention periods separate by a washout. Visit 1: Eligibility (screening, consent/surveys); if eligible, they were randomized and scheduled (~2 weeks) for their Visit 2 with stool collection and diet record deployed for Visit 3 first intervention baseline. Visit 2: Practice/familiarization sessions with EEG cap placement, scheduled ~1 week before to testing visit. Visits 3 and 5: Pre-intervention testing days with the full EEG-based cognitive battery. Visits 4 and 6: Post-intervention follow-ups with the same testing battery. Stools samples were collected over the final 5-days of each intervention period and returned at the subsequent testing visit. (*Figure created using BioRender)*

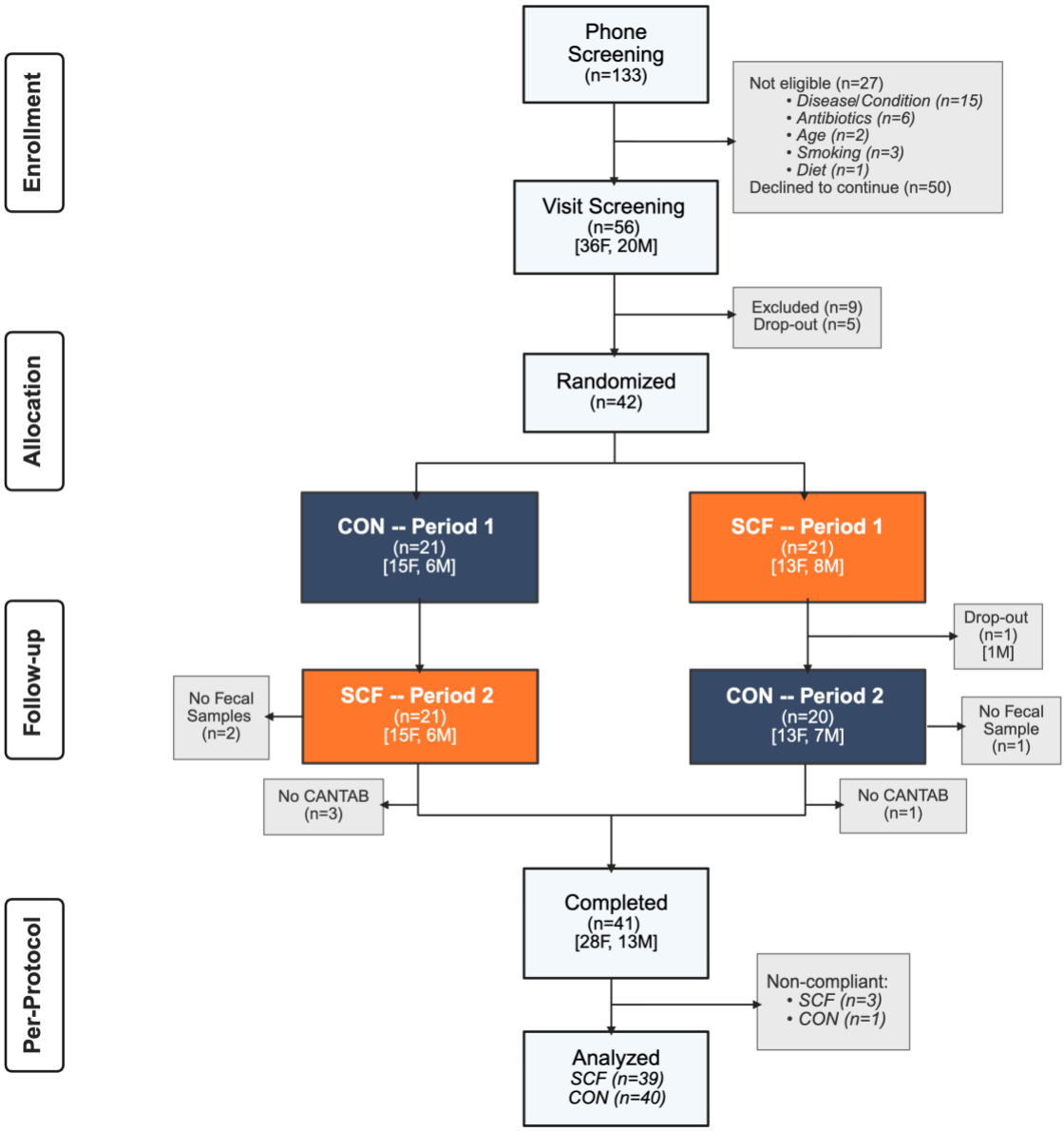

Figure 2. CONSORT flow diagram of recruitment, randomization, and retention. Each "*n*" indicates the number of participants at each stage of the study. Participants were randomized to maltodextrin (CON) or soluble corn fiber (SCF) in a counterbalanced crossover design. (*Figure created using BioRender)*

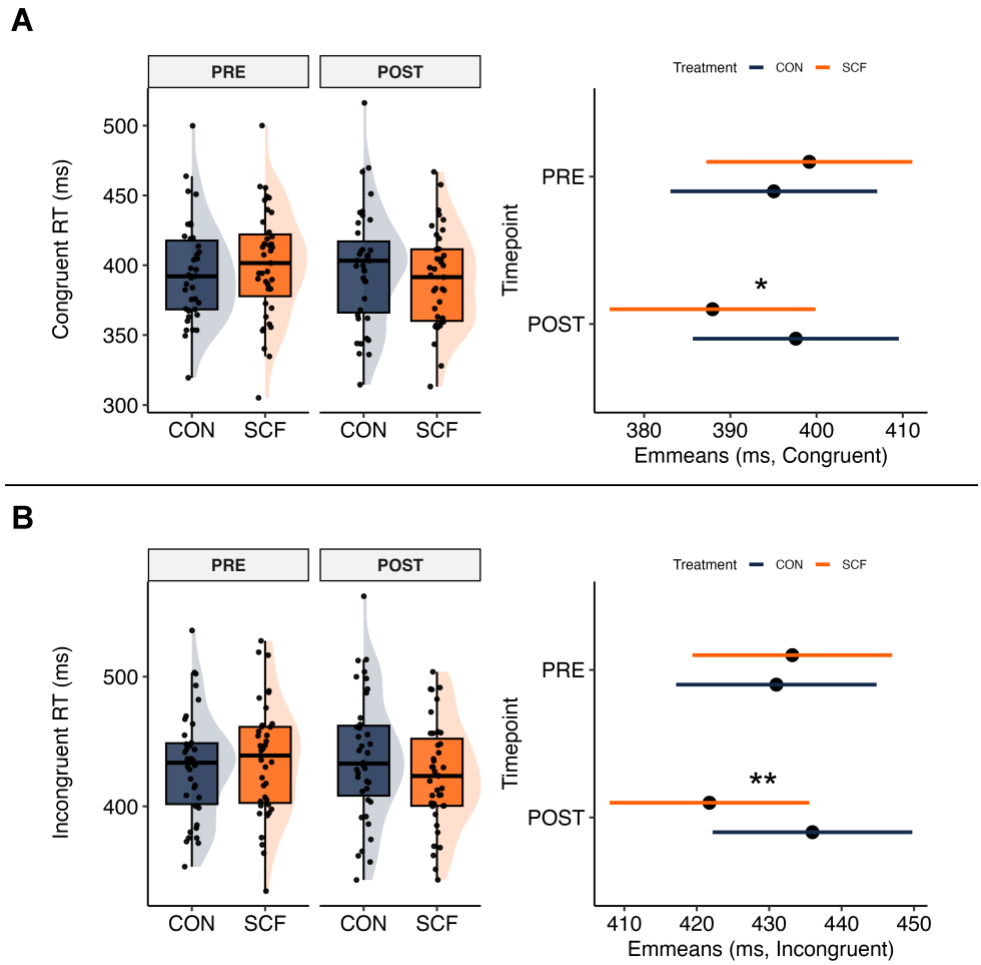

Figure 3. Flanker task reaction times for both congruencies across each timepoint. Raw distributions (left) and model-derived estimated marginal means (right) of reaction times (RT, ms) are shown for (**A**) congruent trials (top row) and (**B**) incongruent trials (bottom row) across treatment and time. Statistical significance derived from *post-hoc* pairwise comparisons. FDR-adjusted *p*-values annotated as follows: ** < 0.01; * < 0.05; † < 0.1.

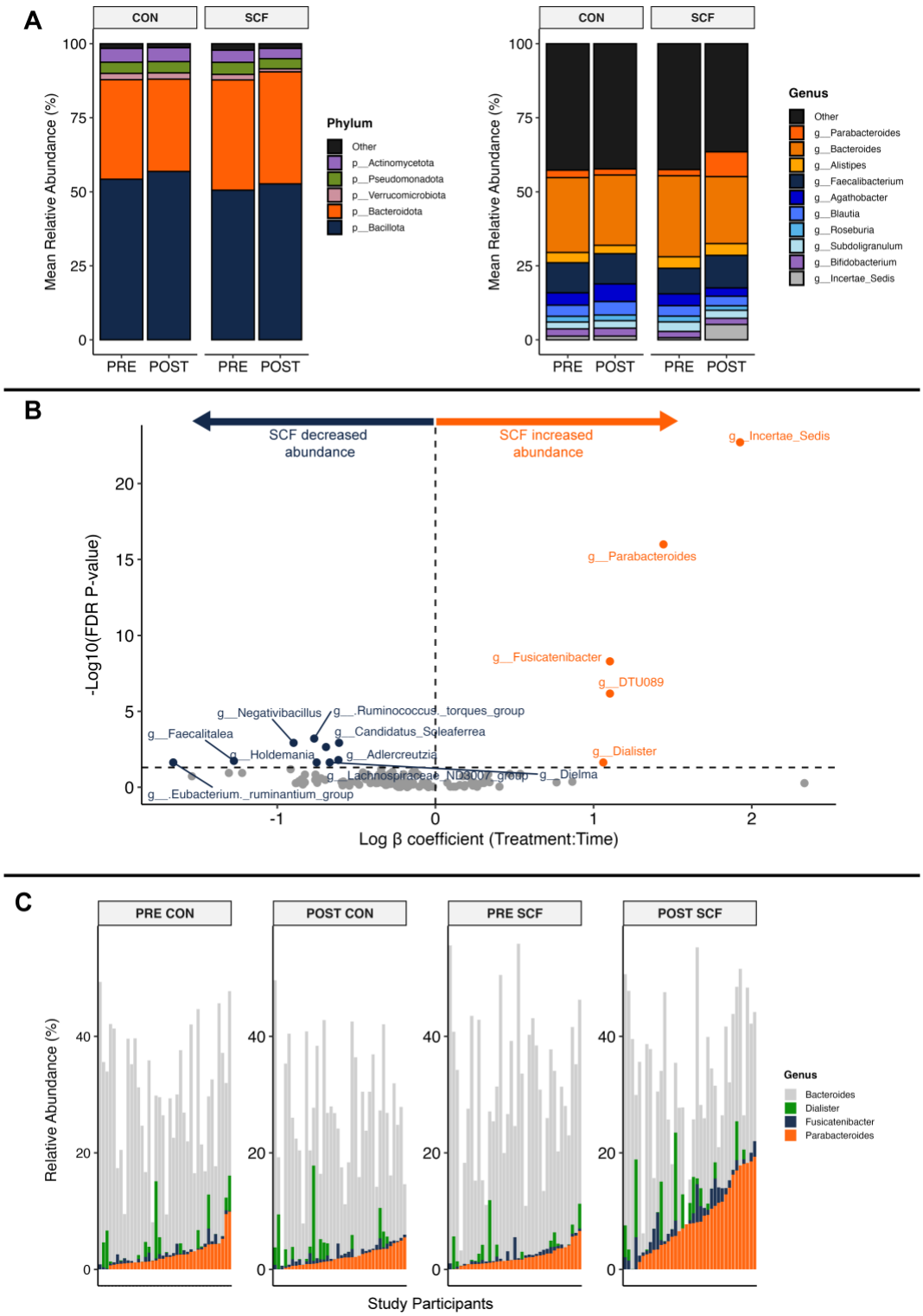

Figure 4. 16S microbiota composition across condition and participants. (**A**) First row shows relative abundance (%) of the top 5 for phyla (left) and top 10 for genera (right) across the interventions averaged within conditions. Color gradient for genera correspond to their parent phylum. (**B**) 16S differential abundance volcan plot shows glmm model interaction estimates with effect size increasing from the center dashed vertical line). The y-axis corresponds to the significance of the genera, higher meaning more significant, with a horizontal dashed line indicating the FDR $p = 0.05$ threshold. The waterfall plot (**C**) highlights patterns from statistically relevant genera at the individual level.

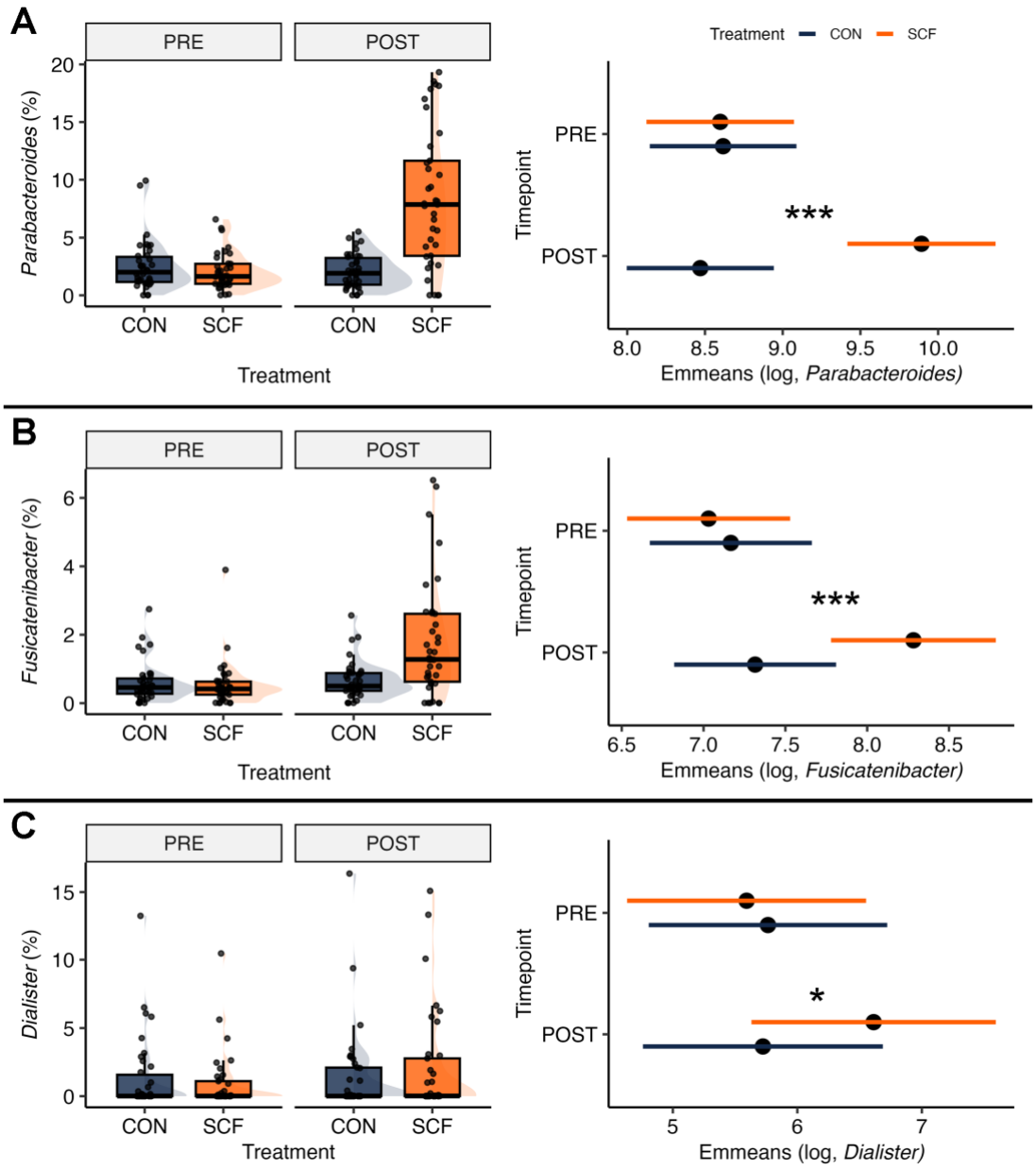

Figure 5. Distribution and *post-hoc* comparison of 16S selected genera. Relative abundances (% of sequences) on the left and estimated marginal pairwise comparisons (Emmeans, right; log scale) of *Parabacteroides* (A), *Fusicatenibacter* (B), and *Dialister* (C) across conditions. *Post-hoc* analyses show FDR-adjusted *p* between treatment at endpoint. Statistical significance is annotated as follows: *** < 0.001; ** < 0.01; * < 0.05; † < 0.1.

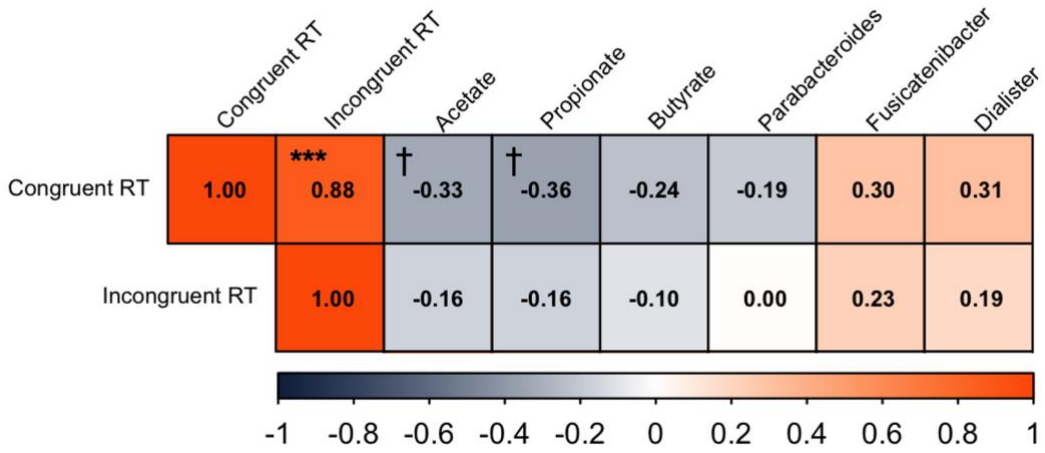

Figure 6. Spearman correlation heatmap of reaction times, fecal SCFAs, and 16S genera following soluble corn fiber intervention. Heatmap displays Spearman's coefficients (ρ) between the markers of interest and the flanker task reaction times ($n = 37$; SCF arm only). Positive correlations are orange, negative correlations blue, with intensity reflecting the magnitude. Spearman p-values were FDR adjusted. Statistical significances are annotated as follows: p *** < 0.001, † < 0.1.

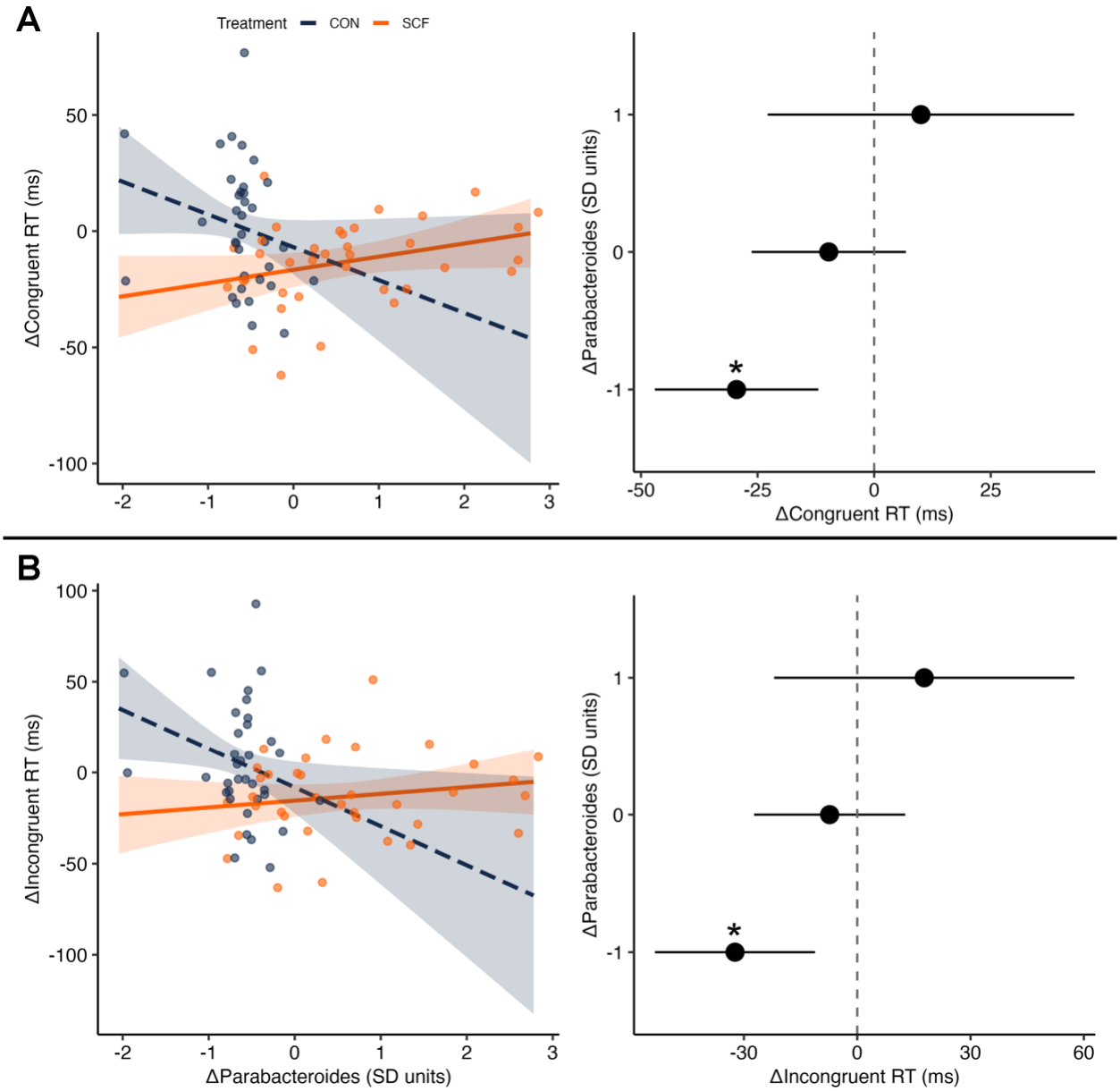

Figure 7. Interaction between 16S *Parabacteroides* and SCF effect on RTs. Moderation outcomes, with the top row (**A**) for congruent RTs, and the bottom row (**B**) for incongruent RTs (ΔRT, ms) plotted as a function of change in the relative abundance of *Parabacteroides* (centered and scaled). On the left, lines represent model-predicted simple slopes for maltodextrin (blue) and SCF (orange) groups with vertical dotted lines marking the conditional effects at low (-1 standard deviation (SD)), centered mean, and high (+1 SD) of Δ*Parabacteroides*. On the right, panels show estimated pairwise differences (SCF-CON) from emmeans contrasts of the moderator values; the vertical line indicates no change, crossing indicates no statistical significance. Significance threshold p * <0.05.

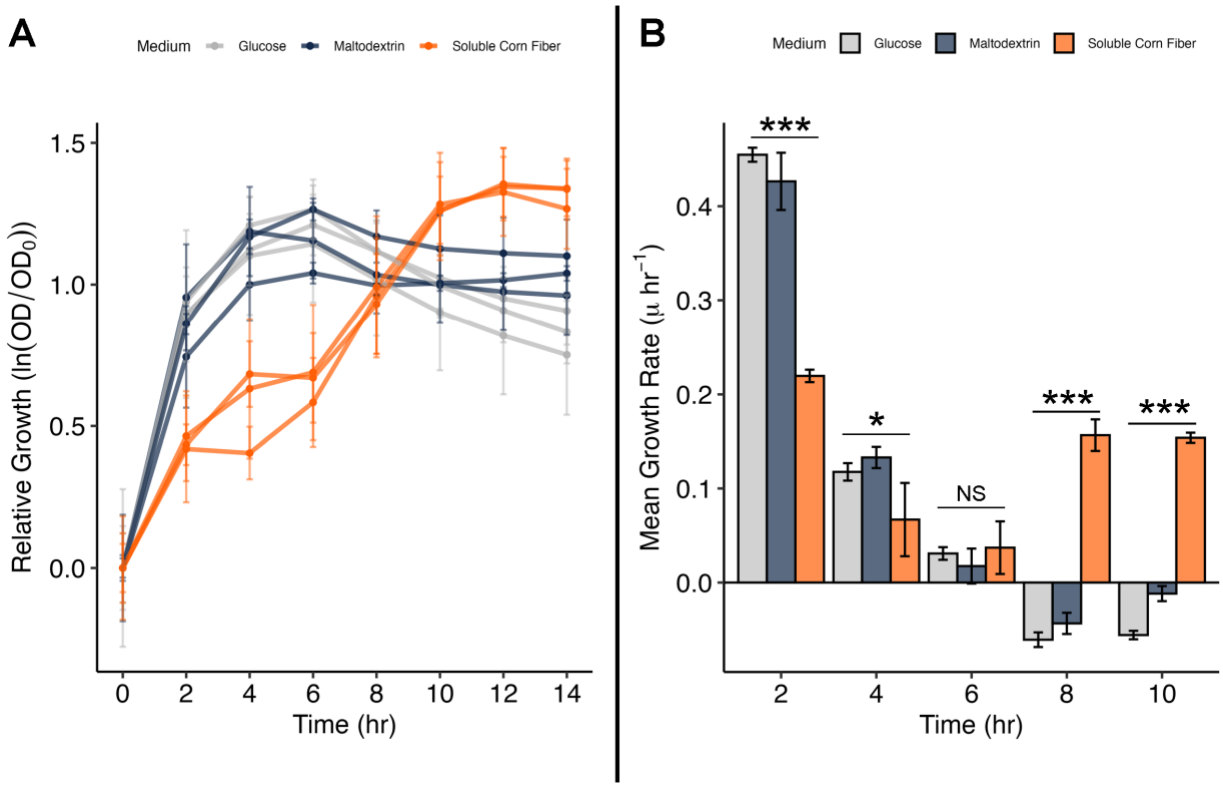

Figure 8. Growth rates of *Parabacteroides distasonis* cultured in M9 supplement with SCF compared to controls. The relative log growth curve of *P. distasonis* (A) in M9 minimal medium supplemented with different carbohydrate sources. OD_0 represents the initial optical density (OD_{600}) at time zero. Each curve represents a mean biological replicate (N = 3), and error bars indicate propagated standard deviations. The mean growth rate (B), calculated as the slope of ln(OD) over sequential 2-hour intervals, cut off at 10-hrs. Bars represent average growth rate across replicates. Significance threshold *p*: '***' < 0.001, '**' < 0.01, '*' < 0.05, '†' < 0.1, 'NS' > 0.1.

Figure 9. Abundance of carbohydrate metabolism-associated gene families comparison between responders and non-responders at endpoint of the SCF intervention. Heatmap displaying the abundance of carbohydrate metabolism-related gene families annotated by HUMAnNv3.0 across six participants (N = 6), stratified by responder (R1–R3) and non-responder (NR1–NR3) status. Genes families shown (rows) were selected from a total of 1,180 unique carbohydrate-associated gene families based on a $\log_2$ fold change > 2 in mean abundance between responders and non-responders [log2(R/NR)]. The top 40 gene families are presented. Abundance values were row-scaled using Z-score normalization to emphasize relative variation across samples. Orange indicates higher abundance, and blue indicates lower abundance for each gene.

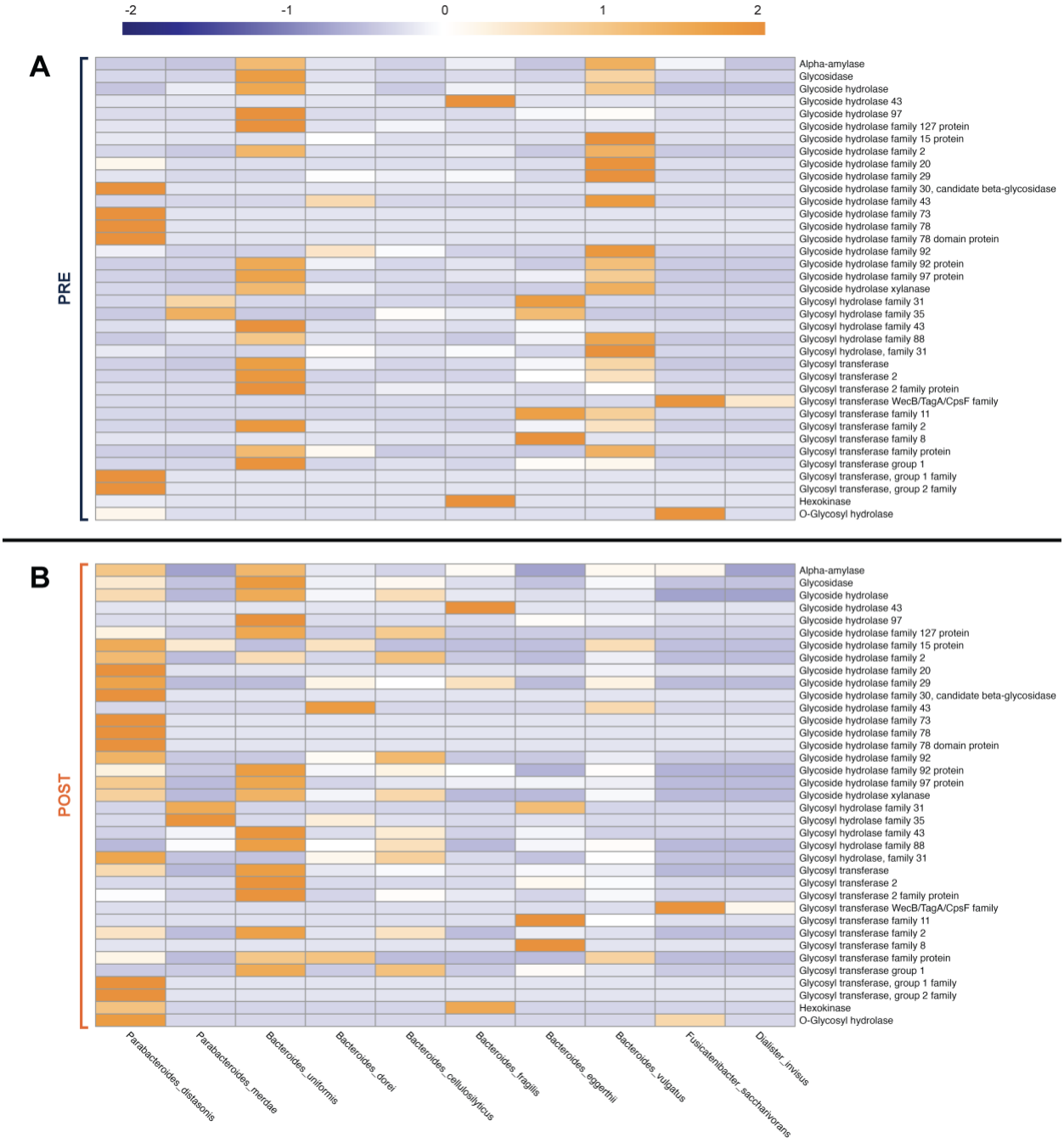

Figure 10. Responders' species-level profile contributions over time to carbohydrate metabolism gene family abundances. Heatmaps showing the contribution of individual species (columns) to the abundance of 40 carbohydrate metabolism-associated gene families (rows) of microbial responders. The top panel (A) shows the baseline timepoint while the bottom panel (B) shows the endpoint of the SCF intervention. Gene abundance was row-normalized using Z-scores to highlight species-level contributions, with orange indicating higher and blue indicating lower abundance for each gene.